2017-07-01

Blending and Mixed Variational Principles to Overcome Locking Phenomena in Isogeometric Beams

Kyle Dennis Richardson
Brigham Young University

Blending and Mixed Variational Principles to Overcome Locking Phenomena in Isogeometric Beams

Kyle Dennis Richardson

A thesis submitted to the faculty of
Brigham Young University
in partial fulfillment of the requirements for the degree of

Master of Science

Michael A. Scott, Chair
Fernando S. Fonseca
Paul William Richards

Department of Civil and Environmental Engineering

Brigham Young University

ABSTRACT

Blending and Mixed Variational Principles to Overcome Locking Phenomena in Isogeometric Beams

Kyle Dennis Richardson
Department of Civil and Environmental Engineering, BYU
Master of Science

Two methods for overcoming locking phenomena in isogeometric beams are presented. The first method blends the rotation of a Timoshenko beam with the rotation of a Bernoulli beam to produce realistic displacements in straight beams. The second method uses mixed variational principles, specifically the Hu-Washizu Principle, to produce realistic displacements as well as realistic strains without post-processing.

Keywords: Isogeometric Analysis, IGA, locking free, blended, Timoshenko, Bernoulli, beams, linear analysis, Hu-Washizu, mixed variational

ACKNOWLEDGMENTS

I first would like to thank my parents. They have always provided me the support and help that I have needed in my life. I know I would not have made it here without them. I would also like to thank all of the members of the BYU IGA group. I don't think we would have figured out some of the finer details without them. I would especially like to thank Dr. Michael Scott. I didn't even know that work like this existed until that day when he stopped in the hall and asked if I wanted to do research with him.

TABLE OF CONTENTS

LIST OF TABLES

LIST OF FIGURES

NOMENCLATURE

$\tilde{\mathbf{X}}$	Undeformed configuration of the beam
$\mathbf{X}$	Beam centerline in the undeformed configuration
$\tilde{\mathbf{x}}$	Deformed configuration of the beam
$\mathbf{x}$	Beam centerline in the deformed configuration
$\tilde{\mathbf{u}}$	The displacement, i.e. $\tilde{\mathbf{x}} - \tilde{\mathbf{X}}$
$\mathbf{u}$	Beam centerline displacement, i.e. $\mathbf{x} - \mathbf{X}$
$\mathbf{D}_i$	Orthonormal basis where $\mathbf{D}_1$ is the vector perpendicular to cross section in the undeformed configuration, these are often called the directors
$\mathbf{d}_i$	Orthonormal basis where $\mathbf{d}_1$ is the vector perpendicular to cross section in the deformed configuration, these are also often called directors
ξ_i	Curvalinear coordinate system where ξ_1 is the beam centerline parameter
ϕ	The rotation for a planar beam
ε	Axial strain
γ	Shear strain
κ	Curvature or bending strain
$\boldsymbol{\varepsilon}$	The vector of axial, shear, and bending strains
$\boldsymbol{\epsilon}$	The tensor of strains using the symmetric gradient
EA	Axial stiffness
GA	Shear stiffness
EI	Bending stiffness
$\mathbf{C}$	The matrix of stiffness coefficients
$\boldsymbol{\sigma}$	The vector of stress resultants such as the normal force and the shear force
$S(\mathbf{q})$	A function that returns the scalar portion of a quaternion $\mathbf{q}$
$V(\mathbf{q})$	A function that returns the vector portion of a quaternion $\mathbf{q}$
$Q(\mathbf{a})$	A function that returns a quaternion such that $V(Q(\mathbf{a})) = \mathbf{a}$ and $S(Q(\mathbf{a})) = 0$
$\mathbf{e}$	The identity quaternion
δ_{AB}	The Kronecker delta where if $A = B$ then $\delta_{AB} = 1$ and zero otherwise
$\mathbf{E}^e$	The Bézier Extraction Operator associated with element e
$\mathbf{G}^e$	The Gradient Extraction Operator associated with element e
N_A	NURBS basis function A
N_A^{BEZ}	Bernstein basis function A The BEZ comes from that it is also the basis for Bézier curves
λ	A Lagrange Multiplier

Subscripts, superscripts, and other indicators

$[\,]_{,i}$	The derivative with respect to ξ_i
$[\,]_{,s}$	$\frac{[\,]_{,1}}{\|\|\mathbf{X}_{,1}\|\|}$
$[\,]_{,x}$	$[\,]_{,s}$ when the beam is straight and corresponds with the x-axis
$[\,]^{-1}$	The inverse operator
$\delta[\,]$	The first variation
$\Delta[\,]$	The first variation when $\tilde{\mathbf{u}} = \mathbf{0}$
$\bar{[\,]}$	Having to do with the modified strains
$\hat{[\,]}$	Having to do with the unmodified strains
$[\,]^{TIM}$	Having to do with a Timoshenko beam

$[\ ]^{BER}$	Having to do with a Bernoulli beam
$\cdot$	The dot product
$\times$	The cross product
$\otimes$	The Hamiltonian product, used with quaternions

CHAPTER 1. INTRODUCTION

Two methods of alleviating locking are presented in this thesis. The first uses blending to take advantage of the shear locking free behavior of Bernoulli beams while still allowing for the application of the rotational boundary conditions with Timoshenko beams. The second method uses the Hu-Washizu Principle to redefine the strains and eliminate locking completely. Before I delve more into these methods, I present how Isogeometric Analysis (IGA) functions, the beam theory, and what is locking.

1.1 IGA

Traditionally, the Finite Element Method has used linear basis functions to approximate the solution of structural problems. In contrast, IGA uses higher degree basis functions with higher continuity to represent the geometry perfectly and solve for the solution with fewer elements. Various spline basis functions based on Bézier curves, T-splines and more recently U-splines, are used with this goal in mind. However, in this thesis the basis is limited to the NURBS basis. Most of the following overview of NURBS was derived from [1].

NURBS is an acronym for Non-Uniform Rational B-Spline. A spline is a curve that is made up of a sequence of curve segments that are connected together to form a single continuous curve. From now on I will call each curve segment an element as that is essentially what they are in the Finite Element Method. The B-Spline basis is defined by two pieces of information. The first is the degree p while the second is the knot vector. The knot vector contains all of the information needed to define the parametric domain of each element as well as the continuity between the elements. A non-uniform B-Spline is essentially one with elements of varying parametric length. To make it rational, the basis functions just need to be weighted, which allows the representation of more curves. The single element quarter circle in Figure 1.1 can be perfectly represented by the NURBS basis. The entries, or knots, of this knot vector for this curve describes a curve that

parametrically starts at 0 and ends at 1. The repeated zeros say that the start of the curve must match the first control point and the repeated ones say that the end of the curve must match the last control point. Without weights, the circle would not be able to be represented perfectly.

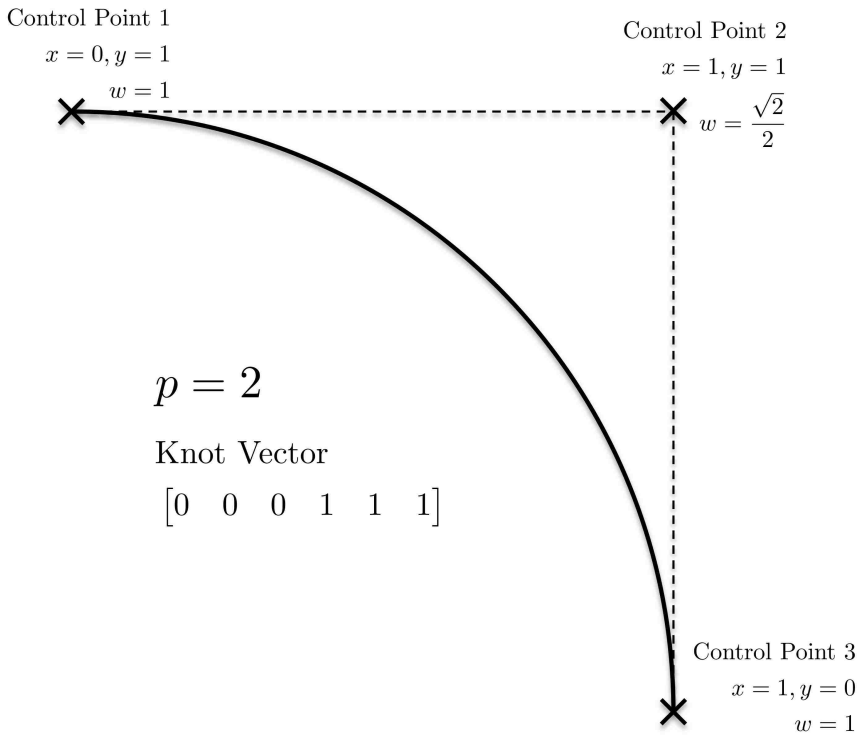

Figure 1.1: A NURBS quarter circle.

Many times in FEA, refinement of the basis functions is desired so that the solution can be better approximated. In traditional FEA this process repeatedly requires approximating the geometry. However, two tools are available that can refine the NURBS basis without modifying the geometry. This means that not only is the basis rich enough to represent geometries exactly, but it can also be refined without modifying these geometries. This avoids the need of reapproximating the geometry. These two tools are degree elevation and knot insertion. Degree elevation basically allows the use of higher degree basis functions, but this cannot be done locally. Degree elevating one portion elevates the entire NURBS. Knot insertion is, however, a local refinement tool. It can be used to split elements and lower continuity. Each knot in the knot vector corresponds to a parameter value on the curve. When a parameter appears in the knot vector for the first time, the

NURBS is split at that point so that the basis has C^{p-1} continuity there. C^d continuity means that the curve and its first d derivatives are continuous at that point. If that parameter appears again the continuity is lowered by one. Knot insertion is the process of adding these parameter values to the knot vector and finding the new control points.

The algorithms for both of these tools can be represented as linear operators. Applying these operators to the control points produces the control points in the new basis such that the geometry is unmodified.

The new basis needs to be represented, as well. This is done by taking advantage of the fact that a C^0 NURBS is equivalent to a set of Bézier curves set end to end. These curves are written in terms of the Bernstein basis, $\mathbf{N}^{BEZ}$. Knot insertion can be used until the basis is C^0. The linear operators that represent these knot insertions are combined together into one operator which is called the Bézier Extraction Operator [2]. Instead of applying the Bézier Extraction Operator to the control points to find the control points in the new basis, like was done during refinement with the other linear operators, it is applied to the easy to evaluate Bernstein basis to find the desired NURBS basis. The Bézier Extraction Operator $\mathbf{E}^e$ is used to define the NURBS basis in the following, where the superscript e specifies which element this operator is for.

$$N_A = \frac{w_A}{w} \sum_B E^e_{AB} N^{BEZ}_B \tag{1.1}$$

where $\frac{w_A}{w}$ is the weighting of the basis function A. Every control point has a weight w_A, and the function w is defined such that the basis forms a partition of unity or they sum to one.

$$w = \sum_A w_A \sum_B E^e_{AB} N^{BEZ}_B \tag{1.2}$$

An example of using the Bézier Extraction Operator can be seen in Figure 1.2. The Bernstein basis for $p = 2$ is evaluated and the knot vector is used to calculate the Bézier Extraction Operators for all three elements.

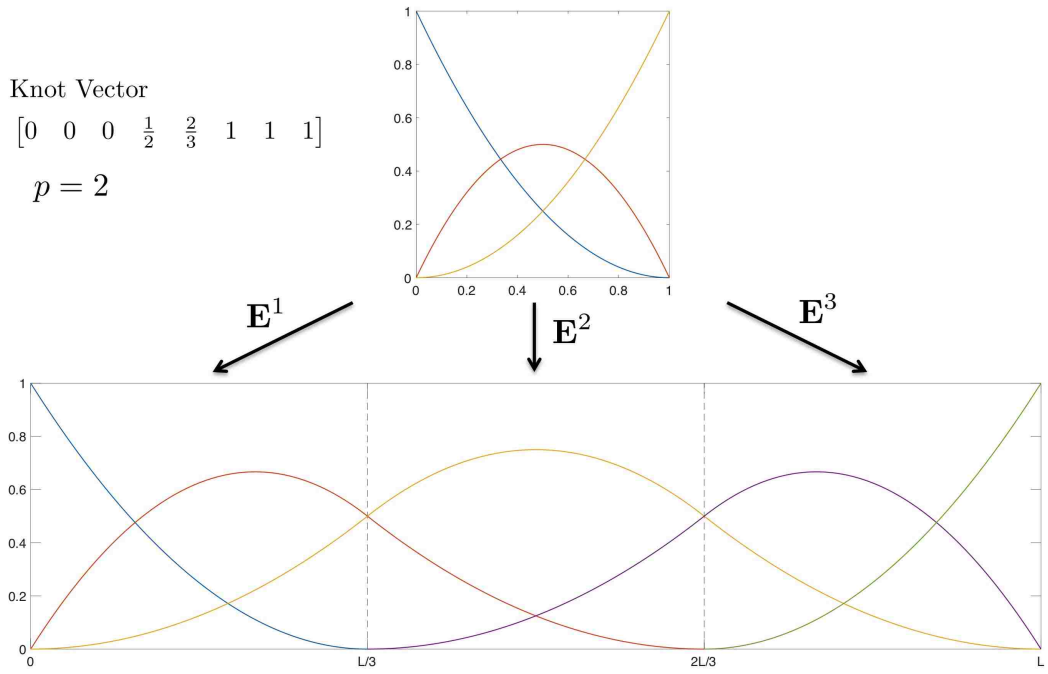

Figure 1.2: An example of using the Bézier Extraction Operator to convert from the Bernstein basis into the NURBS basis.

Using the Bézier Extraction Operator allows IGA to be integrated into the traditional FEA framework. I only need to evaluate the Bernstein Basis once and use this operator to convert it into the required NURBS basis.

1.2 Beam Theory

Appendix A derives a general three dimensional resultant based beam theory, but, for simplicity, I use planar beams throughout the thesis instead of the general three dimensional theory. The reduction of the three dimensional theory to a planar beam an be found there, as well. This leaves only the following three strains.

$$\boldsymbol{\varepsilon} = \begin{bmatrix} \varepsilon \\ \gamma \\ \kappa \end{bmatrix} = \begin{bmatrix} \mathbf{D}_1 \cdot \mathbf{u}_{,s} \\ \mathbf{D}_2 \cdot \mathbf{u}_{,s} - \phi \\ \phi_{,s} \end{bmatrix} \tag{1.3}$$

The variational formulation in this context is

$$\Pi = \frac{1}{2}\int_{\Omega} \boldsymbol{\varepsilon}^T \mathbf{C}\boldsymbol{\varepsilon}\, ds - \Pi_{ext} \tag{1.4}$$

where

$$\Pi_{ext} = \int_{\Omega} (\mathbf{u}\cdot\mathbf{f} + \phi m)\, ds + (\mathbf{u}\cdot\mathbf{R} + \phi M)\Big|_0^L \tag{1.5}$$

where $\mathbf{f}$ is the distributed force, m is the distributed moment, $\mathbf{R}$ is the reaction force, and M is the reaction moment.

For the material moduli, I assume that linear isotropic elastic materials are used. I also assume that the local coordinate system corresponds with the centroidal principal axes. This results in the matrix $\mathbf{C}$ of stiffness coefficients having the following form.

$$\mathbf{C} = \begin{bmatrix} EA & 0 & 0 \\ 0 & GA & 0 \\ 0 & 0 & EI \end{bmatrix} \tag{1.6}$$

The symbol EA is called the axial stiffness, GA the shear stiffness, and EI the bending stiffness.

1.3 Locking Phenomena

Locking is a symptom of the fact that the solution is being discretized with basis functions that are unable to represent the solution exactly. Locking, however, is not a problem until the thickness of the beam is small. Bending of a beam is governed by flexural deformation which results in the magnitude of the deflection being mostly a function of the bending stiffness EI. If a beam is subjected to a load that is a linear function of the bending stiffness, then the displacement does not change by much as the thickness changes. However, as the thickness goes to zero the shear and axial stiffnesses relative to the bending stiffness go to infinity. This emphasizes the inability of the basis functions to represent the shear and axial strains exactly. In the end, the best solution that can be found is one with deformation close to zero as otherwise the energy associated with the axial and shear strains would be unrealistically large.

The canonical example of this is a cantilever Timoshenko beam subject to a moment on the tip which can be seen in Figure 1.3. The calculated tip deflection for this example is seen in

Figure 1.3: The cantilever beam.

Table 1.1. The displacement calculated for $p = 2$ is the correct answer as the exact displacement for this beam can be calculated with basis functions of $p = 2$ [3]. However, the deflection calculated for $p = 1$ is nearly zero. Figure 1.4 shows the calculated shear force for $p = 1$. This illustrates

Table 1.1: Tip Displacement

$p = 1$	0.000012958880353
$p = 2$	0.150000000087715

the problem of oscillating strains caused by basis functions that are unable to represent the strain exactly. The shear strain is produced by two functions that differ by degree and continuity. For

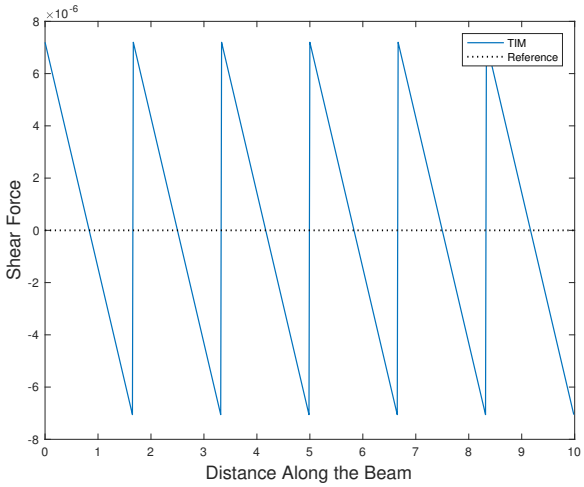

Figure 1.4: The calculated shear force for $p = 1$.

this example the shear stress must be zero, but the two functions together are unable produce the required strain of zero unless they are both equal to zero. So it is seen that the method sacrificed realistic displacements in an attempt to have realistic stresses. This type of locking is called shear locking and it should be noted that Bernoulli beams are shear locking free as the shear strain is set to zero. A Timoshenko beam discretizes the rotation ϕ with the basis functions, but a Bernoulli beam defines ϕ as equal to $\mathbf{D}_2 \cdot \mathbf{u}_{,s}$.

There is another type of locking that is called membrane locking that is related to the fact that for curved beams it is difficult for the basis functions to approximate the axial strain.

Another problem is that even if the displacement is correct, the strains oscillate and produce unrealistic stresses. The stress is often times more important than the displacement. These oscillations can be seen in the computed shear force of the above example in Figure 1.4.

1.4 Removing Locking

Many ways have been presented to alleviate the locking behavior of beams and shells. One extremely popular way is to use reduced quadrature to under-integrate the stiffness. This allows the beam to deflect, but this does not fix the oscillatory nature of the strains. This would need to be fixed through some averaging rule during post-processing.

The purpose of this thesis is to present two methods of alleviating locking behavior. The first method is called blending. It blends the rotation field of a Bernoulli beam with that of a Timoshenko beam so that it is shear locking free, but rotations can be specified or moments can be applied when necessary. This is done by using a Bernoulli beam over the majority of the beam, but using a Timoshenko beam on just the ends so that the rotational boundary conditions can be applied. The second method is more general in that it can remove all locking behavior including oscillating strains. It uses the Hu-Washizu Principle to redefine the strains into the proper basis so as to prevent locking and oscillations. This method is called the mixed displacement method. Both methods are general principles that can be applied to other types of structural elements such as non-planar beams and shells.

CHAPTER 2. BLENDING

I first remove shear locking through the use of blending. Blending is a manner of combining multiple fields together into one. I use blending to combine the rotations of a Timoshenko beam on the ends of the beam with the rotations of a Bernoulli beam on the interior of the beam. This is because Bernoulli beams are free of shear locking, but it is hard to apply rotational boundary conditions to them. Using a Timoshenko beam on just the ends allows these conditions to be easily applied while still avoiding the shear locking that a Timoshenko beam experiences.

This method is an application to beams of the work presented for shells in [4]. The use of a Gradient Extraction Operator was especially inspired by that work.

2.1 Definition of Blending

Before I present the full application of blending to the rotation fields of a beam, I present a simple example of blending together the two cubic Bézier curves that can be seen in Figure 2.1. For a field to be blended it must first be written in terms of a sum of basis functions and control

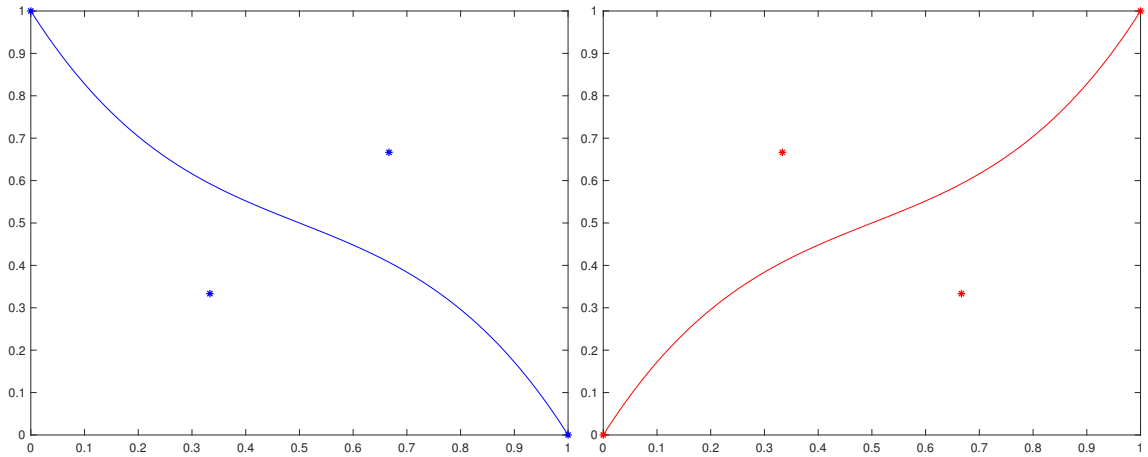

(a) Curve A (b) Curve B

Figure 2.1: The two curves to be blended and their control points.

points. The two curves I blend together are written in such a form.

$$A = \sum_i N_i A_i \qquad B = \sum_i N_i B_i \tag{2.1}$$

Blending is then performed by specifying nodes as coming from one curve or another. In this example I specify the nodes as either A nodes or B nodes. They have to be one or the other. The sum is then performed over this new set of nodes in the following manner where C is the blended curve. Nodes 1 and 2 are specified to be A nodes and Nodes 3 and 4 to be B nodes.

$$C = \sum_{i \in A} N_i A_i + \sum_{i \in B} N_i B_i \tag{2.2}$$

The resulting curve is displayed in Figure 2.2. This curve mostly follows Curve A near the start,

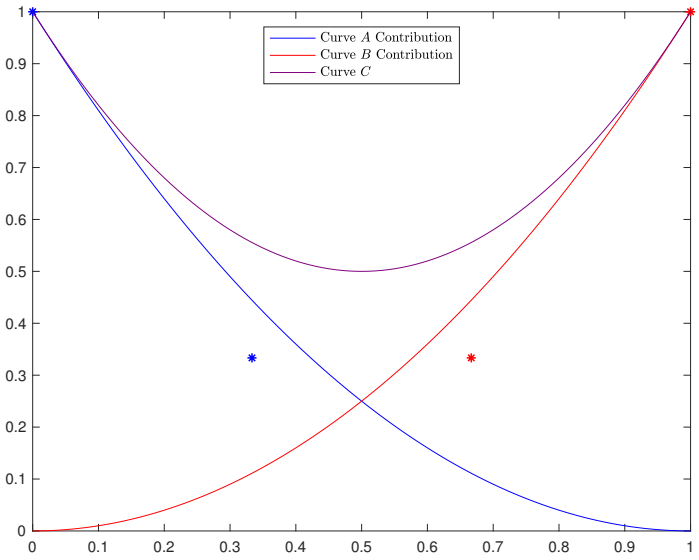

Figure 2.2: The contributions of the two curves and the resultant blended curve.

but by the end it is following Curve B. This happens because the basis functions are chosen such that the curve mimics the positions of the control points. The NURBS basis also has this property.

2.2 Gradient Extraction Operator

The need for the Gradient Extraction Operator $\mathbf{G}^e$ arises from the fact that many fields that need to be blended together are written in terms of the derivative of the basis functions instead of the basis functions. The rotation for a Bernoulli beam is an example of this.

$$\phi^{BER} = u_{,x} = \sum_A N_{A,x} u_A = \frac{1}{\left\|\mathbf{X}_{,1}\right\|} \sum_A N_{A,1} u_A \tag{2.3}$$

This operator provides a way to write the derivative of the basis functions in terms of the basis functions and thus know what the different control points are that need to be mixed together in the blending process. For Bézier curves this is fairly easily done as the derivative of any non-rational Bézier curve can be represented by a Bézier curve of one degree lower. Using degree elevation one can then write this new curve in terms of the original basis. This produces a linear operator to which the Bézier Extraction Operator can then be applied to produce the B-spline Gradient Extraction Operator. The derivatives for NURBS can be represented by a simple modification of this linear operator to produce a non-linear operator. This means that any field that is written in terms of the derivative of the NURBS basis can also be written in terms of the same NURBS basis instead.

$$N_{A,1} = \sum_B G^e_{AB} N_B \tag{2.4}$$

This is visualized by a quadratic B-Spline in Figure 2.3. The NURBS Gradient Extraction Operator is defined as the following

$$G^e_{AB} = -\frac{w_{,1}}{w}\delta_{AB} + \frac{w_A}{w_B} \sum_C \sum_D E^e_{AC} G^{BEZ}_{CD} E^{e-1}_{DB} \tag{2.5}$$

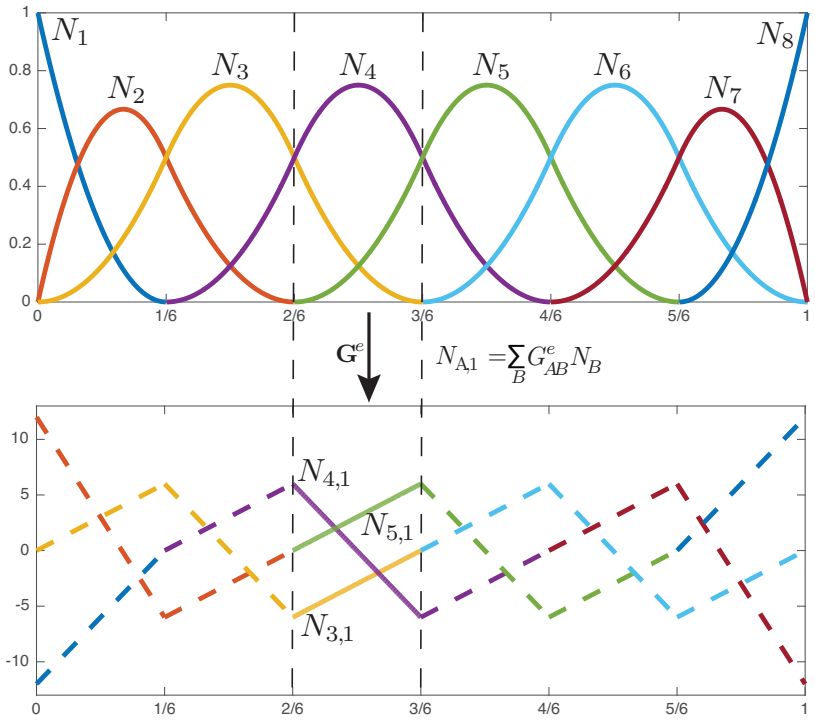

Figure 2.3: Visualization of the how the Gradient Extraction Operator works.

where $\mathbf{E}^e$ is the Bezier Extraction Operator and $\mathbf{G}^{BEZ}$ is the Non-Rational Bezier Gradient Extraction Operator defined as follows

$$G^{BEZ}_{AB} = \frac{1}{t_1 - t_0} \begin{cases} 2B - p - 2 & \text{if } A = B \\ 1 - B & \text{if } A = B - 1 \\ p + 1 - B & \text{if } A = B + 1 \\ 0 & \text{otherwise} \end{cases} \tag{2.6}$$

where t_0 is the value of the parameter ξ_1 at the start of the element and t_1 at the end. Also in Equation 2.5, the expression E^{e-1}_{DB} refers to the entry DB of the inverse of the operator $\mathbf{E}^e$

2.3 Blending of the Rotation Fields

The Timoshenko rotation is already in terms of the basis while the Bernoulli rotation can now be written in terms of the basis.

$$\phi^{TIM} = \sum_{A} N_A \phi_A \tag{2.7}$$

$$\phi^{BER} = \frac{1}{\left\|\mathbf{X}_{,1}\right\|} \sum_{A} \sum_{B} G^{e}_{AB} u_A N_B \tag{2.8}$$

Blending is done by specifying nodes as either Timoshenko or Bernoulli nodes. The rotation ϕ is then found by summing over the basis functions. If it is a Timoshenko node then the Timoshenko term associated with that node's basis function is added and the same goes for the Bernoulli nodes.

$$\phi = \sum_{A \in TIM} N_A \phi_A + \frac{1}{\left\|\mathbf{X}_{,1}\right\|} \sum_{B \in BER} \sum_{C \in All} u_C G^{e}_{CB} N_B \tag{2.9}$$

This definition can now be used in the definitions of strain in the Finite Element Method. Because C^1 basis functions are required for Bernoulli beams they are also required for Blended beams.

2.4 Matrix Formulation

The linear system can be written as

$$\mathbf{KU} = \mathbf{F} \tag{2.10}$$

where

$$\mathbf{K} = \left[\mathbf{K}_{AB}\right] \quad \mathbf{U} = \{\mathbf{U}_A\} \quad \mathbf{F} = \{\mathbf{F}_A\} \tag{2.11}$$

and

$$\mathbf{K}_{AB} = \int_{\Omega} \mathbf{B}_A^T \mathbf{C} \mathbf{B}_B \, ds \tag{2.12}$$

$$\mathbf{C} = \begin{bmatrix} GA & 0 \\ 0 & EI \end{bmatrix} \tag{2.13}$$

$$\mathbf{B}_A = \begin{bmatrix} N_{A,s} - \frac{1}{||\mathbf{X}_{,1}||} \sum_B G^e_{AB} N_B & -N_A \delta_{AC} \\ \left(\frac{1}{||\mathbf{X}_{,1}||} \sum_B G^e_{AB} N_B \right)_{,s} & N_{A,s} \delta_{AC} \end{bmatrix} \tag{2.14}$$

$$\mathbf{U}_A = \begin{bmatrix} u_A \\ \phi_A \end{bmatrix} \tag{2.15}$$

where the subscript B belongs to the set of Bernoulli nodes and the subscript C to the set of Timoshenko nodes.

2.5 Examples

I here present the results of the same beam under several different boundary conditions and loadings. In all cases, the beam is discretized with 6 elements. The maximum deflections of the beam for all cases are presented in the following sections. Results for traditional Timoshenko beams, traditional Bernoulli beams, and Blended beams are compared for several different degrees. There are no solutions for the Bernoulli beams and the Blended beams when $p = 1$ as C^1 basis functions are required. The results show that shear locking is limited while still allowing for the application of rotational boundary conditions.

Figure 2.4 shows the distribution of the different types of nodes for the $p = 2$ case. Notice that only the end nodes are specified as Timoshenko nodes. The other cases are similar in that only the end nodes are specified as Timoshenko nodes.

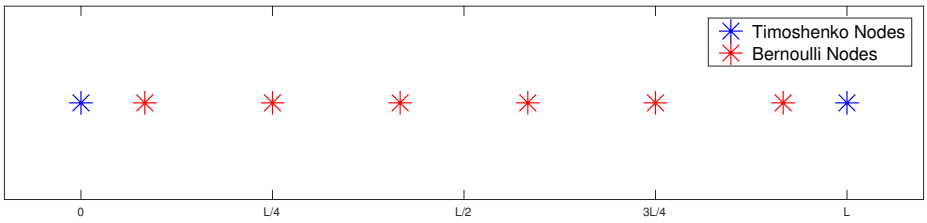

Figure 2.4: The distribution of node types for the $p = 2$ case.

2.5.1 Simply Supported Beam

In the first example a simply supported beam is used, which can be seen in Figure 2.5. The

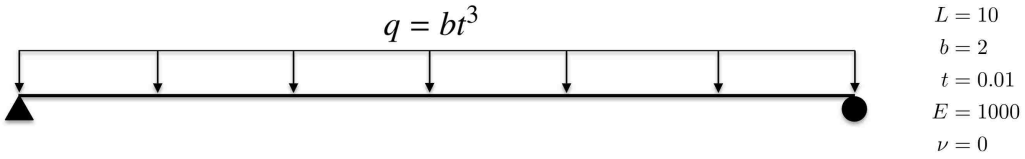

Figure 2.5: The simply supported beam.

analytic solution for this beam is $u \approx 1.56$ [5]. The results are presented in Table 2.1. Locking is extreme in the case of the Timoshenko beam where $p = 1$, but is alleviated in the case of higher degrees, although it is still present due to the differing continuity and degrees. At $p = 4$, the beam unlocks as the basis functions are now rich enough to represent the deflection exactly [3]. The Bernoulli and Blended beams suffered from almost no locking.

Table 2.1: Maximum deflection of the simply supported beam.

	Timoshenko	Bernoulli	Blended
$p = 1$	0.00013198885536	N/A	N/A
$p = 2$	1.25108734162825	1.52777777777777	1.52777999999921
$p = 3$	1.35273881489767	1.56250000000000	1.56250082638114
$p = 4$	1.56250299987632	1.56249999999999	1.56250066581014

2.5.2 Fixed Fixed Beam

The second example is similar to the first one in that the end rotations are constrained to zero. This can be seen in Figure 2.5. The analytic solution is $u \approx 0.3125$ [6]. The results are

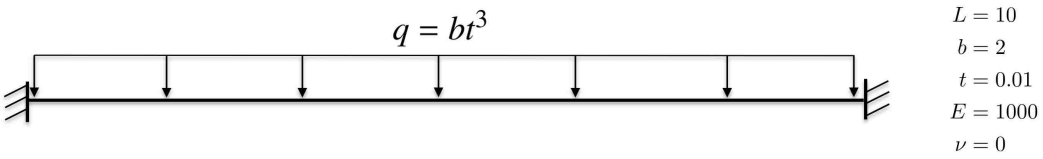

Figure 2.6: The fixed fixed beam.

presented in Table 2.2. This example is harder to set up as the end rotations for a Bernoulli beam have to be set over multiple nodes. This isn't the case for the Timoshenko or Blended beams. The results are similar to the previous example.

Table 2.2: Maximum deflection of the fixed fixed beam.

	Timoshenko	Bernoulli	Blended
$p = 1$	0.000026997926579	N/A	N/A
$p = 2$	0.001087341652665	0.277777777777778	0.277779999973334
$p = 3$	0.102738814889438	0.312500000000000	0.312500826385418
$p = 4$	0.312502999998129	0.312499999999999	0.312500665793884

2.5.3 Cantilever Beam

The last example is a cantilever beam with traction boundary conditions applied to the other end. The tractions are such that the displacement curve is the same as the previous example. This requires a point load of $\frac{qL}{2}$ and a moment of $\frac{qL^2}{12}$ [6]. This can be seen in Figure 2.7. The results are presented in Table 2.3. This examples does not include results for a Bernoulli beam as applying moment tractions are even harder to apply than rotation boundary conditions.

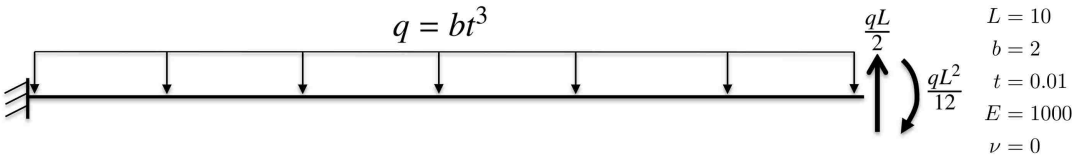

Figure 2.7: The cantilever beam.

Table 2.3: Maximum deflection of the cantilever beam.

	Timoshenko	Blended
$p = 1$	0.000029997667402	N/A
$p = 2$	0.001087341652727	0.277779999973333
$p = 3$	0.102738814901887	0.312500826385421
$p = 4$	0.312503000023566	0.312500665793880

In Figure 2.8 I look at the number of DOFs needed by the two types of beams to achieve the maximum reference displacement for this last example. The regular Timoshenko beam needs more than twice as many DOFs as the blended beam.

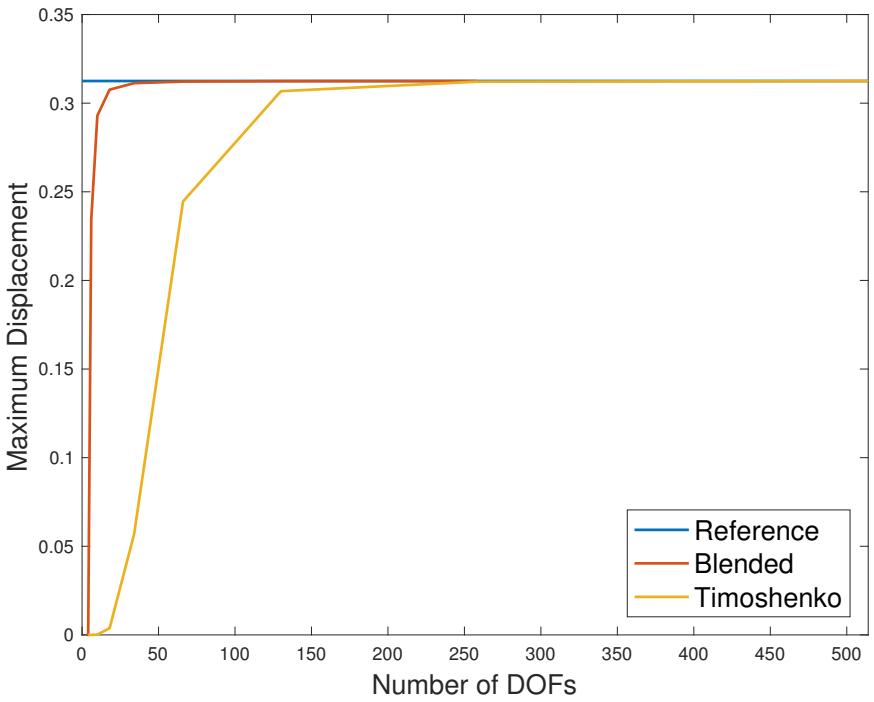

Figure 2.8: The maximum displacement versus the number of DOFs for $p = 2$.

CHAPTER 3. THE MIXED DISPLACEMENT METHOD

The second method, known as the mixed displacement method, is capable of eliminating all locking including oscillating strains. This is an application of the work presented for shells in [5] and a good overview of the Hu-Washizu Principle can be found in [7].

3.1 The Hu-Washizu Principle

The Hu-Washizu Principle is a three field approach that uses the fields stress $\boldsymbol{\sigma}$, strain $\boldsymbol{\varepsilon}$, and displacement $\mathbf{u}$ instead of just the displacement field that the traditional form uses.

$$\Pi_{HW}(\mathbf{u},\boldsymbol{\varepsilon},\boldsymbol{\sigma}) = \frac{1}{2}\int_{\Omega} \boldsymbol{\varepsilon}^T \mathbf{C}\boldsymbol{\varepsilon}\, ds + \int_{\Omega} \boldsymbol{\sigma}^T(\boldsymbol{\varepsilon}(\mathbf{u}) - \boldsymbol{\varepsilon})\, ds - \Pi_{ext} \tag{3.1}$$

This formulation avoids locking by using the stress as a Lagrange Multiplier to equate the actual strain, $\boldsymbol{\varepsilon}$, to the strain from the displacement, $\boldsymbol{\varepsilon}(\mathbf{u})$ [7], but only in an average sense. This allows both the strain and the displacement to be realistic without introducing spurious energy terms due to using basis functions to approximate the solution.

Equation 3.1 can be reduced to a two field approach by saying $\boldsymbol{\sigma} = \mathbf{C}\boldsymbol{\varepsilon}$ and because of my assumptions I can say that $\mathbf{C} = \mathbf{C}^T$. The weak form of this can be seen in the following.

$$\delta\Pi_{HW} = -\int_{\Omega} \delta\boldsymbol{\varepsilon}^T \mathbf{C}\boldsymbol{\varepsilon}\, ds + \int_{\Omega} \delta\boldsymbol{\varepsilon}^T \mathbf{C}\boldsymbol{\varepsilon}(\mathbf{u})\, ds + \int_{\Omega} \delta\boldsymbol{\varepsilon}(u)^T \mathbf{C}\boldsymbol{\varepsilon}\, ds - \delta\Pi_{ext} = 0 \tag{3.2}$$

This can also be written in block matrix form to maintain the basic structure of an FEM program.

$$\delta\Pi_{HW} = \int_{\Omega} \begin{bmatrix} \delta\boldsymbol{\varepsilon}(\mathbf{u}) \\ \delta\boldsymbol{\varepsilon} \end{bmatrix}^T \begin{bmatrix} \mathbf{0} & \mathbf{C} \\ \mathbf{C} & -\mathbf{C} \end{bmatrix} \begin{bmatrix} \boldsymbol{\varepsilon}(\mathbf{u}) \\ \boldsymbol{\varepsilon} \end{bmatrix} ds - \delta\Pi_{ext} = 0 \tag{3.3}$$

I now split the strains into two sets; those that lock, $\bar{\boldsymbol{\varepsilon}}$, and those that don't, $\hat{\boldsymbol{\varepsilon}}$. The same splitting is done for $\boldsymbol{\varepsilon}(\mathbf{u})$. The first set is represented by a new auxiliary field while for the other set I say $\hat{\boldsymbol{\varepsilon}} = \hat{\boldsymbol{\varepsilon}}(\mathbf{u})$. The matrix $\mathbf{C}$ must also be subdivided into the following.

$$\mathbf{C} = \begin{bmatrix} \hat{\bar{\mathbf{C}}} & \mathbf{0} \\ \mathbf{0} & \bar{\bar{\mathbf{C}}} \end{bmatrix} \tag{3.4}$$

Applying these modifications, Equation 3.3 is rewritten into the following.

$$\delta\Pi_{HW} = \int_{\Omega} \begin{bmatrix} \delta\hat{\boldsymbol{\varepsilon}}(\mathbf{u}) \\ \delta\bar{\boldsymbol{\varepsilon}}(\mathbf{u}) \\ \delta\bar{\boldsymbol{\varepsilon}} \end{bmatrix}^T \begin{bmatrix} \hat{\bar{\mathbf{C}}} & \mathbf{0} & \mathbf{0} \\ \mathbf{0} & \mathbf{0} & \bar{\bar{\mathbf{C}}} \\ \mathbf{0} & \bar{\bar{\mathbf{C}}} & -\bar{\bar{\mathbf{C}}} \end{bmatrix} \begin{bmatrix} \hat{\boldsymbol{\varepsilon}}(\mathbf{u}) \\ \bar{\boldsymbol{\varepsilon}}(\mathbf{u}) \\ \bar{\boldsymbol{\varepsilon}} \end{bmatrix} ds - \delta\Pi_{ext} = 0 \tag{3.5}$$

3.2 Modified Strains

The two main sources of locking are shear locking and membrane locking due to the inaccuracies of the approximated shear and axial strains, respectively. These strains can be replaced with new fields which are defined as the derivative of what are called the $\bar{u}$ fields. Each $\bar{u}$ field is discretized in terms of the basis functions and there is one for each component of the modified strains. With this definition, it can be seen that the strain lives in the space of the derivative of the displacement field. This is where it should be as the strain is basically a derivative of the displacement. This is why it is called the mixed displacement method.

There is a problem with the use of the $\bar{u}$ fields in that only their derivatives are used. This leaves a constant that corresponds with a zero energy mode that must be restrained. I can do this by setting one node to zero. I, however, add a constraint that the $\bar{u}$ fields must average to zero over the beam. This is done because methods independent of the discretization and boundary are desired

for shells. This constraint is applied using Lagrange Multipliers for which I use the symbol λ. The method of setting one node to zero would be more efficient.

3.3 Straight Timoshenko Beams

To examine the method in the context of shear locking, I only consider straight beams which lie along the x-axis subject to vertical loads. This leaves only the following two strains

$$\begin{bmatrix} \gamma \\ \kappa \end{bmatrix} = \begin{bmatrix} u_{,x} - \phi \\ \phi_{,x} \end{bmatrix} \tag{3.6}$$

I modify the shear strain by introducing a single auxiliary displacement variable, or $\bar{u}$ field, such that

$$\bar{\gamma} = \bar{u}_{,x} \tag{3.7}$$

3.3.1 Variational Formulation

The variational formulation in this simple context becomes

$$\begin{aligned} \Pi = &\frac{1}{2}\int_\Omega \phi_{,x} EI \phi_{,x}\, dx - \frac{1}{2}\int_\Omega \bar{u}_{,x} GA \bar{u}_{,x}\, dx \\ &+ \int_\Omega \bar{u}_{,x} GA (u_{,x} - \phi)\, dx + \lambda \int_\Omega \bar{u}\, dx - \Pi_{ext} \end{aligned} \tag{3.8}$$

and the corresponding weak form is

$$\begin{aligned} \delta\Pi = &\int_\Omega \delta\phi_{,x} EI \phi_{,x}\, dx - \int_\Omega \delta\bar{u}_{,x} GA \bar{u}_{,x}\, dx \\ &+ \int_\Omega \delta\bar{u}_{,x} GA (u_{,x} - \phi)\, dx + \int_\Omega \bar{u}_{,x} GA (\delta u_{,x} - \delta\phi)\, dx \\ &+ \delta\lambda \int_\Omega \bar{u}\, dx + \lambda \int_\Omega \delta\bar{u}\, dx - \delta\Pi_{ext} = 0 \end{aligned} \tag{3.9}$$

3.3.2 Euler-Lagrange Equations

The Euler-Lagrange equations are

$$\delta u: \quad GA\bar{\gamma}_{,x} + q = 0 \quad \text{on } \Omega \tag{3.10}$$

$$GA\bar{\gamma} - V = 0 \quad \text{on } \Gamma \tag{3.11}$$

$$\delta \phi: \quad EI\kappa_{,x} + GA\bar{\gamma} + m = 0 \quad \text{on } \Omega \tag{3.12}$$

$$EI\kappa - M = 0 \quad \text{on } \Gamma \tag{3.13}$$

$$\delta \bar{u}: \quad GA\gamma_{,x} - GA\bar{\gamma}_{,x} - \lambda = 0 \quad \text{on } \Omega \tag{3.14}$$

$$GA\gamma - GA\bar{\gamma} = 0 \quad \text{on } \Gamma \tag{3.15}$$

$$\delta \lambda: \quad \int_{\Omega} \bar{u}\, dx = 0. \tag{3.16}$$

It can be seen that the new shear strains take the place of the traditional shear strain in this set of constraints. There are also constraints that equate the two shear strains to each other. These constraints are not strong enough to reintroduce locking as they are more of constraints in an average sense.

3.3.3 Discretization

The unknown fields u, $\bar{u}$, and ϕ are discretized as

$$u \approx u^h = \sum_A N_A u_A \tag{3.17}$$

$$\bar{u} \approx \bar{u}^h = \sum_A N_A \bar{u}_A \tag{3.18}$$

$$\phi \approx \phi^h = \sum_A N_A \phi_A \tag{3.19}$$

3.3.4 Matrix Formulation

The linear system can be written as

$$\begin{bmatrix} \mathbf{K} & \mathbf{B}_\lambda \\ \mathbf{B}_\lambda^T & 0 \end{bmatrix} \begin{bmatrix} \mathbf{U} \\ \lambda \end{bmatrix} = \begin{bmatrix} \mathbf{F} \\ 0 \end{bmatrix} \tag{3.20}$$

where

$$\mathbf{K} = \left[\mathbf{K}_{AB}\right] \quad \mathbf{B}_\lambda = \{\mathbf{B}_\lambda^A\} \tag{3.21}$$

$$\mathbf{U} = \{\mathbf{U}_A\} \quad \mathbf{F} = \{\mathbf{F}_A\} \tag{3.22}$$

and

$$\mathbf{K}_{AB} = \int_\Omega \mathbf{B}_A^T \mathbf{C} \mathbf{B}_B \, ds \tag{3.23}$$

$$\mathbf{B}_\lambda^A = \int_\Omega \begin{bmatrix} 0 \\ 0 \\ N_A \end{bmatrix} ds \tag{3.24}$$

$$\mathbf{C} = \begin{bmatrix} 0 & 0 & GA \\ 0 & EI & 0 \\ GA & 0 & -GA \end{bmatrix} \tag{3.25}$$

$$\mathbf{B}_A = \begin{bmatrix} N_{A,s} & -N_A & 0 \\ 0 & N_{A,s} & 0 \\ 0 & 0 & N_{A,s} \end{bmatrix} \tag{3.26}$$

$$\mathbf{U}_A = \begin{bmatrix} u_A \\ \phi_A \\ \bar{u}_A \end{bmatrix} \tag{3.27}$$

3.4 Curved Bernoulli Beams

In the context of Bernoulli beams, $\phi = \mathbf{D}_2 \cdot \mathbf{u}_{,s}$, which means that the shear strain is zero and shear locking is eliminated. This allows the study of only membrane locking. The resulting strains are

$$\begin{bmatrix} \varepsilon \\ \kappa \end{bmatrix} = \begin{bmatrix} \mathbf{D}_1 \cdot \mathbf{u}_{,s} \\ (\mathbf{D}_2 \cdot \mathbf{u}_{,s})_{,s} \end{bmatrix} \tag{3.28}$$

I modify the axial strain by introducing a single auxiliary displacement variable, or $\bar{u}$ field, such that

$$\bar{\varepsilon} = \bar{u}_{,s} \tag{3.29}$$

3.4.1 Variational Formulation

The variational formulation becomes

$$\begin{aligned} \Pi = \frac{1}{2}\int_\Omega \kappa EI\kappa\, ds - \frac{1}{2}\int_\Omega \bar{\varepsilon} EA\bar{\varepsilon}\, ds \\ + \int_\Omega \bar{\varepsilon} EA\varepsilon\, ds + \lambda \int_\Omega \bar{u}\, ds - \Pi_{ext} \end{aligned} \tag{3.30}$$

and the corresponding weak form is

$$\begin{aligned} \delta\Pi = \int_\Omega \delta\kappa EI\kappa\, ds - \int_\Omega \delta\bar{\varepsilon} EA\bar{\varepsilon}\, ds \\ + \int_\Omega \delta\bar{\varepsilon} EA\varepsilon\, ds + \int_\Omega \delta\varepsilon EA\bar{\varepsilon}\, ds \\ + \delta\lambda \int_\Omega \bar{u}\, ds + \lambda \int_\Omega \delta\bar{u}\, ds - \delta\Pi_{ext} = 0 \end{aligned} \tag{3.31}$$

3.4.2 Euler-Lagrange equations

The Euler-Lagrange equations are

$$(\delta\mathbf{u}\cdot\mathbf{D}_1): \quad EA\bar{\varepsilon}_{,s} - (\mathbf{D}_1\cdot\mathbf{D}_{2,s})(EI\phi_{,ss}+m)+n=0 \quad \text{on } \Omega \tag{3.32}$$

$$EA\bar{\varepsilon} - N = 0 \quad \text{on } \Gamma \tag{3.33}$$

$$(\delta\mathbf{u}\cdot\mathbf{D}_2): \quad (\mathbf{D}_2\cdot\mathbf{D}_{1,s})(EA\bar{\varepsilon}) - (EI\phi_{,sss}+m_{,s})+v=0 \quad \text{on } \Omega \tag{3.34}$$

$$EI\phi_{,ss}+m+V=0 \quad \text{on } \Gamma \tag{3.35}$$

$$\delta\phi: \quad EI\phi_{,s} - M = 0 \quad \text{on } \Gamma \tag{3.36}$$

$$\delta\bar{u}: \quad EA\varepsilon_{,s} - EA\bar{\varepsilon}_{,s} - \lambda = 0 \quad \text{on } \Omega \tag{3.37}$$

$$EA\varepsilon - EA\bar{\varepsilon} = 0 \quad \text{on } \Gamma \tag{3.38}$$

$$\delta\lambda: \quad \int_\Omega \bar{u}\,ds = 0 \tag{3.39}$$

where N is the axial force, V is the transverse shear force, M is the end moment, n is the distributed axial force, v is the distributed transverse force, and m is the distributed moment. Again, this new strain, which in this case is the axial strain, takes the place of the traditional strain in this set of constraints. These two axial strains are also constrained so that they are equivalent in an average sense.

3.4.3 Discretization

The unknown fields $\mathbf{u}$ and $\bar{u}$ are discretized as

$$\mathbf{u} \approx \mathbf{u}^h = \sum_A N_A \mathbf{u}_A \tag{3.40}$$

$$\bar{u} \approx \bar{u}^h = \sum_A N_A \bar{u}_A \tag{3.41}$$

3.4.4 Matrix Formulation

The linear system can be written as

$$\begin{bmatrix} \mathbf{K} & \mathbf{B}_\lambda \\ \mathbf{B}_\lambda^T & 0 \end{bmatrix} \begin{bmatrix} \mathbf{U} \\ \lambda \end{bmatrix} = \begin{bmatrix} \mathbf{F} \\ 0 \end{bmatrix} \tag{3.42}$$

where

$$\mathbf{K} = \left[\mathbf{K}_{AB}\right] \quad \mathbf{B}_\lambda = \{\mathbf{B}_\lambda^A\} \tag{3.43}$$

$$\mathbf{U} = \{\mathbf{U}_A\} \quad \mathbf{F} = \{\mathbf{F}_A\} \tag{3.44}$$

and

$$\mathbf{K}_{AB} = \int_\Omega \mathbf{B}_A^T \mathbf{C} \mathbf{B}_B \, ds \tag{3.45}$$

$$\mathbf{B}_\lambda^A = \int_\Omega \begin{bmatrix} \mathbf{0} \\ N_A \end{bmatrix} ds \tag{3.46}$$

$$\mathbf{C} = \begin{bmatrix} 0 & 0 & EA \\ 0 & EI & 0 \\ EA & 0 & -EA \end{bmatrix} \tag{3.47}$$

$$\mathbf{B}_A = \begin{bmatrix} \mathbf{D}_1^T N_{A,s} & 0 \\ \mathbf{D}_2^T N_{A,ss} + \mathbf{D}_{2,s}^T N_{A,s} & 0 \\ \mathbf{0} & N_{A,s} \end{bmatrix} \tag{3.48}$$

$$\mathbf{U}_A = \begin{bmatrix} \mathbf{u}_A \\ \bar{u}_A \end{bmatrix} \tag{3.49}$$

3.5 Numerical Examples

3.5.1 Simply-Supported Straight Timoshenko Beam

A straight simply supported beam is considered under a distributed load. This beam and its parameters can be seen in Figure 3.1 and it is analyzed using various thicknesses t. The analytical value of the mid-beam deflection is $u \approx 1.56$ [5] and the shear force $V = \frac{qL}{2} - qx$. In all cases, the beam is discretized with 6 elements and the calculated shear force is normalized by the analytic reaction force $\frac{qL}{2}$.

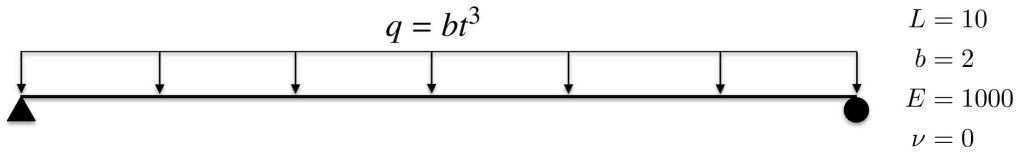

Figure 3.1: The simply supported beam.

In the following plots, I denote a standard displacement-based Timoshenko beam by TIM and the mixed displacement Timoshenko beam by TIM MD. Figure 3.2 shows that shear locking is eliminated in all cases by the mixed displacement method. As the beam goes thin, the displacement goes to zero for the traditional method while the mixed displacement method does not experience locking at all, independent of the thickness. The beam with $p = 1$ is especially susceptible to locking using the traditional method, but unlocks using the mixed displacement method. Higher degree beams exhibit locking to a lesser degree until $p = 4$ when the exact solution can be represented. Figure 3.4 shows that the analytic stress resultants are recovered while the traditional methods produce oscillating stress resultants. Figure 3.3 shows that the $\bar{u}$ field for the shear strain averages to zero in all cases as specified by the added constraint to eliminate the zero energy mode.

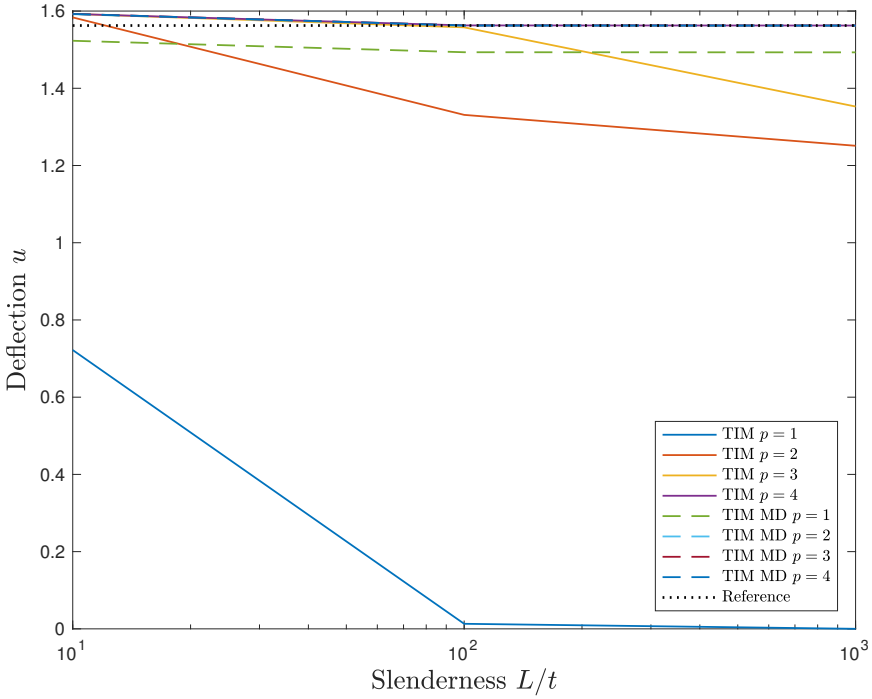

Figure 3.2: Comparison of TIM and TIM MD for several degrees and thicknesses.

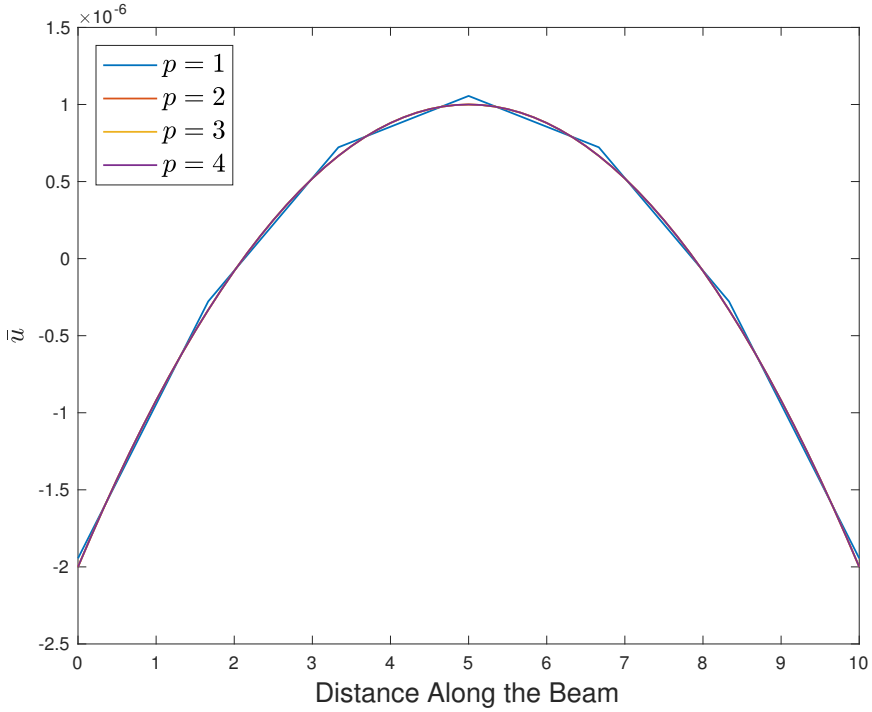

Figure 3.3: The computed TIM MD $\bar{u}$ for several degrees and $\frac{L}{t} = 1000$.

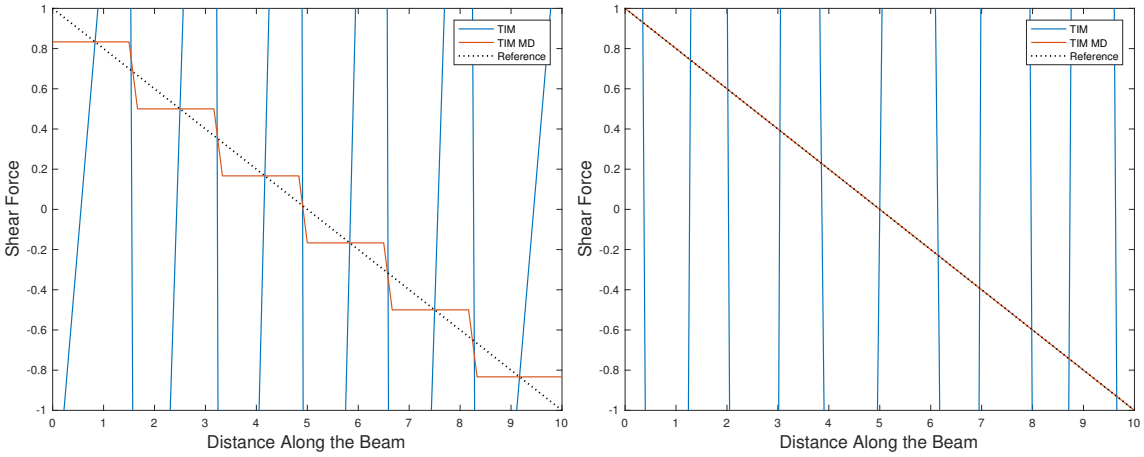

(a) Normalized shear force with $p = 1$ and $\frac{L}{t} = 1000$

(b) Normalized shear force with $p = 2$ and $\frac{L}{t} = 1000$

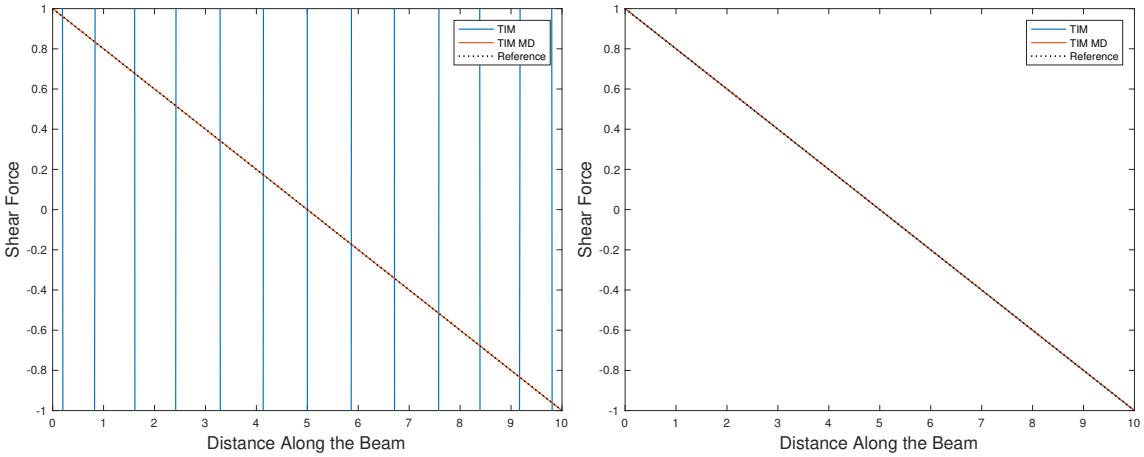

(c) Normalized shear force with $p = 3$ and $\frac{L}{t} = 1000$

(d) Normalized shear force with $p = 4$ and $\frac{L}{t} = 1000$

Figure 3.4: A comparison of computed shear forces for TIM and TIM MD for different degrees and $\frac{L}{t} = 1000$.

3.5.2 Curved Cantilever Bernoulli Beam

A curved cantilever beam is considered under the action of a point load in the radial direction. This beam can be seen in Figure 3.5 and it is analyzed with various thicknesses t. The analytic value of the transverse tip deflection is $u \approx 0.942$ [5] and the analytic axial force is $N = F\cos\frac{s}{R}$. In all cases, the beam is discretized with 10 elements and the axial force is normalized by the point load F. In the plots, I denote a standard displacement-based Bernoulli beam by BER and the mixed displacement Bernoulli beam by BER MD. Figure 3.6 shows that membrane locking is eliminated in all cases by the mixed displacement method. The traditional method deflects less as the beam goes thin while the mixed displacement method does not experience locking. Figure 3.8 shows that the analytic stress resultants are recovered the traditional methods produce oscillating results. Figure 3.7 shows that the $\bar{u}$ field for the axial strain averages to zero in all cases.

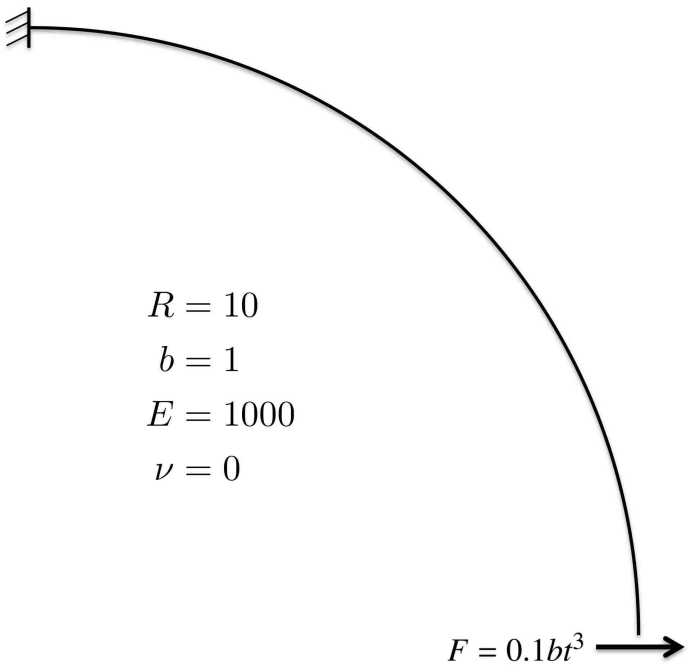

Figure 3.5: The curved cantilever beam.

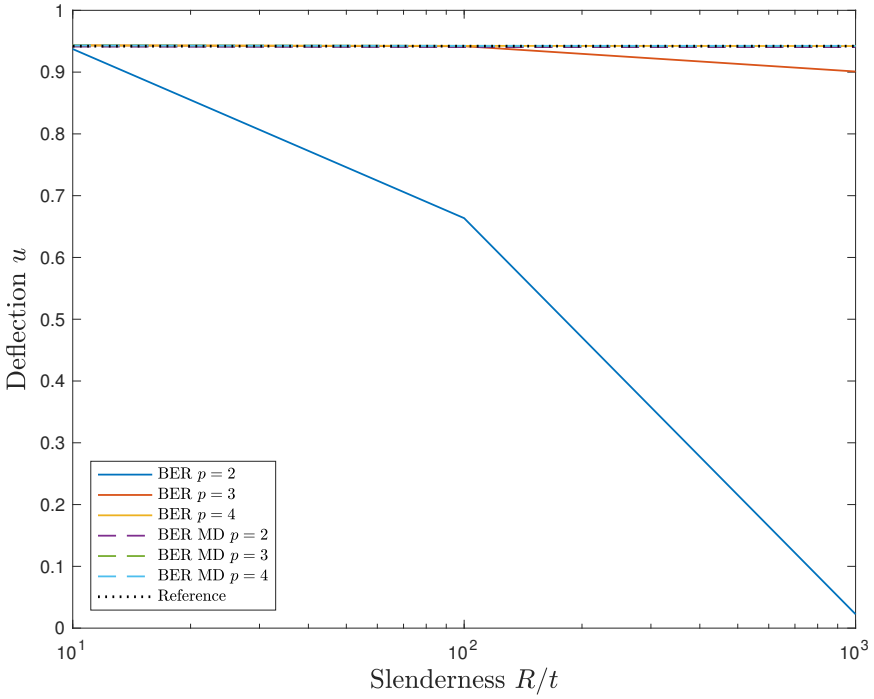

Figure 3.6: Comparison of BER and BER MD for several degrees and thicknesses.

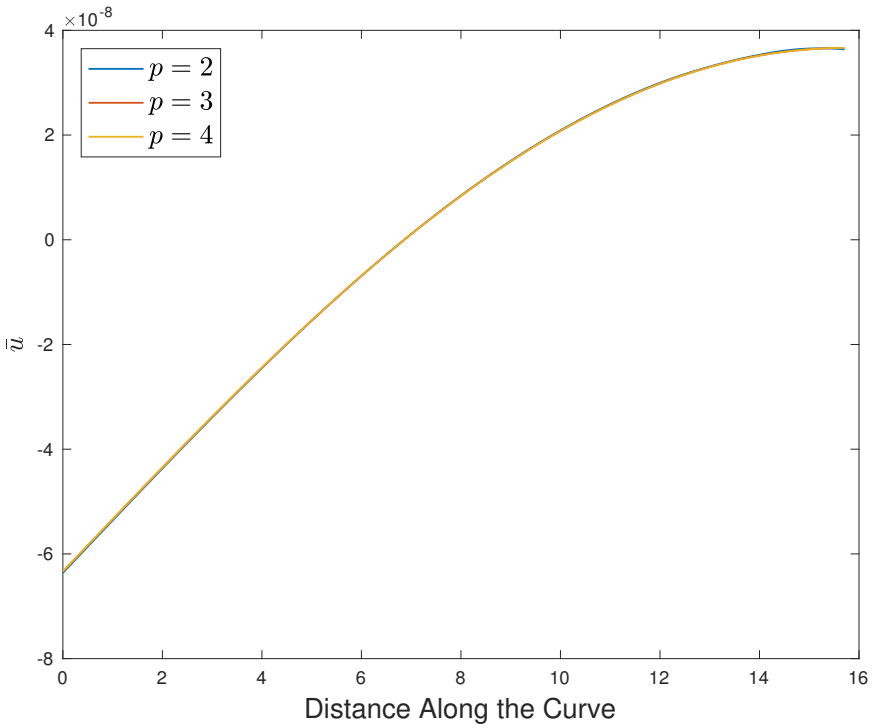

Figure 3.7: The computed BER MD $\bar{u}$ for several degrees and $\frac{R}{t} = 1000$.

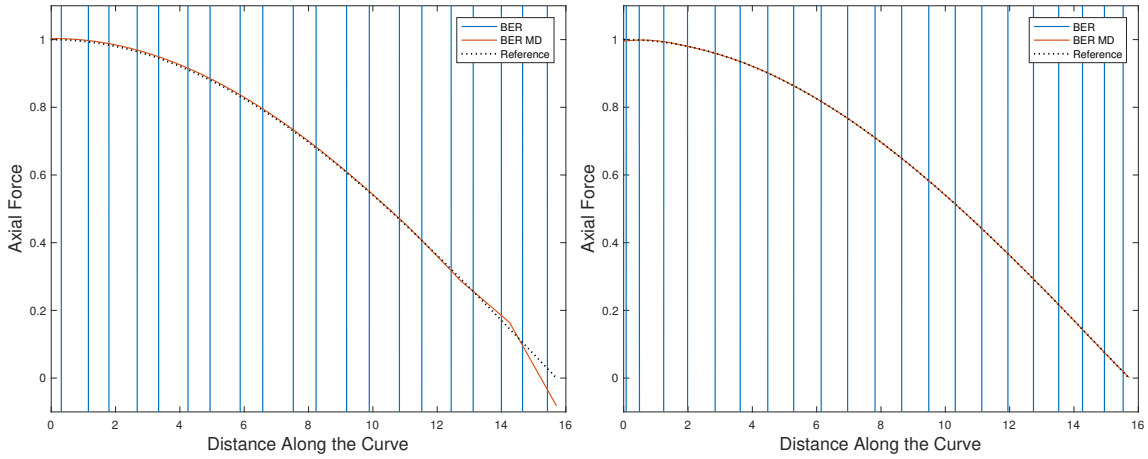

(a) Normalized axial force with $p = 2$ and $\frac{R}{t} = 1000$

(b) Normalized axial force with $p = 3$ and $\frac{R}{t} = 1000$

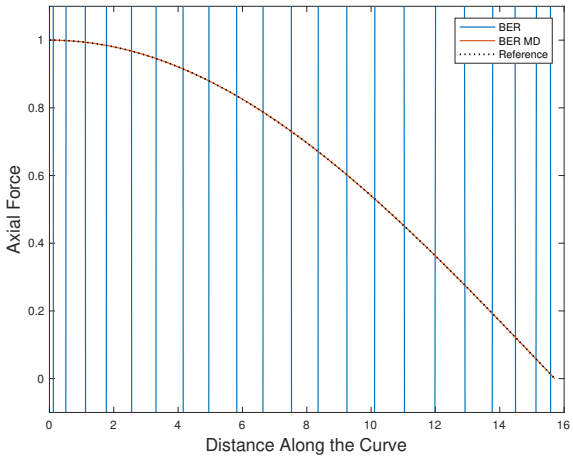

(c) Normalized axial force with $p = 4$ and $\frac{R}{t} = 1000$

Figure 3.8: A comparison of computed axial forces for BER and BER MD for different degrees and $\frac{R}{t} = 1000$.

3.5.3 Curved Cantilever Timoshenko Beam

The curved cantilever beam problem is repeated using a Timoshenko beam instead of a Bernoulli beam to demonstrate that the mixed displacement method can eliminate combined membrane and shear locking. Auxiliary displacement variables, or $\bar{u}$ fields, are defined for both the axial strain and the shear strain. Figure 3.9 shows that shear and membrane locking are eliminated in all cases when the mixed displacement method is used. The traditional method produces deflections that tend towards zero as the beam goes thin, but the mixed displacement method produces the correct displacement independent of the thickness. Figure 3.12 and Figure 3.13 show that the analytic axial and shear stress resultants are recovered while the traditional method produces oscillating stress resultants. Figure 3.10 and Figure 3.11 show that both of the $\bar{u}$ fields average to zero as specified by the added constraint.

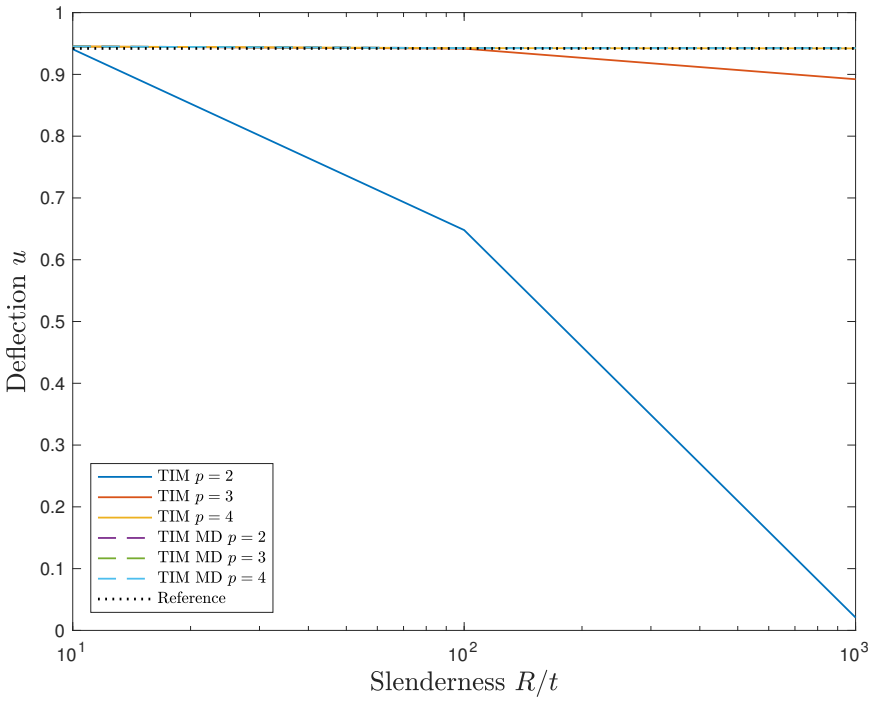

Figure 3.9: A comparison of TIM and TIM MD for several degrees and thicknesses.

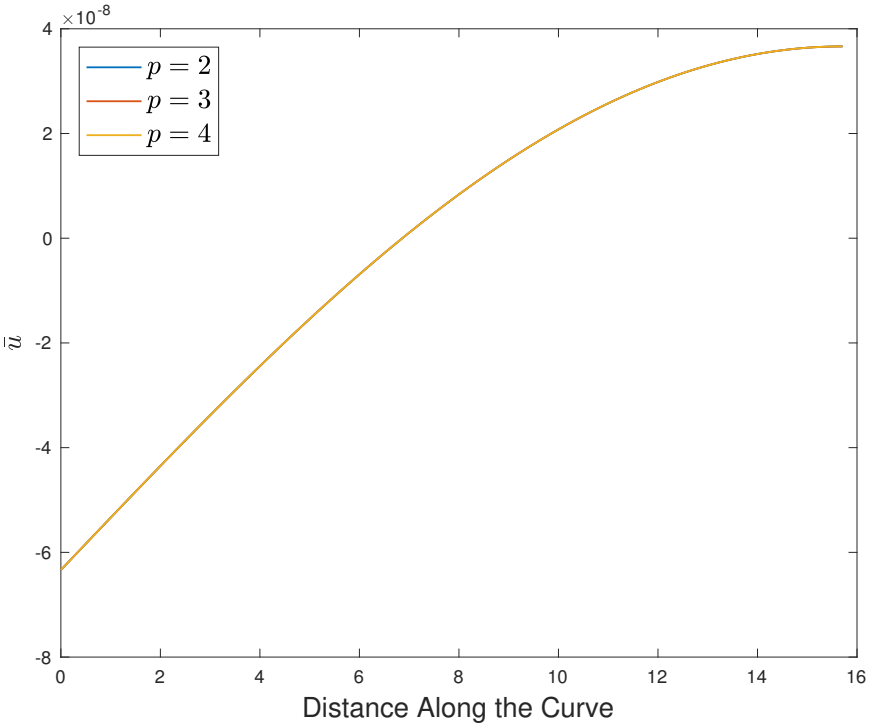

Figure 3.10: The computed TIM MD $\bar{u}$ for axial strain for several degrees and $\frac{R}{t} = 1000$.

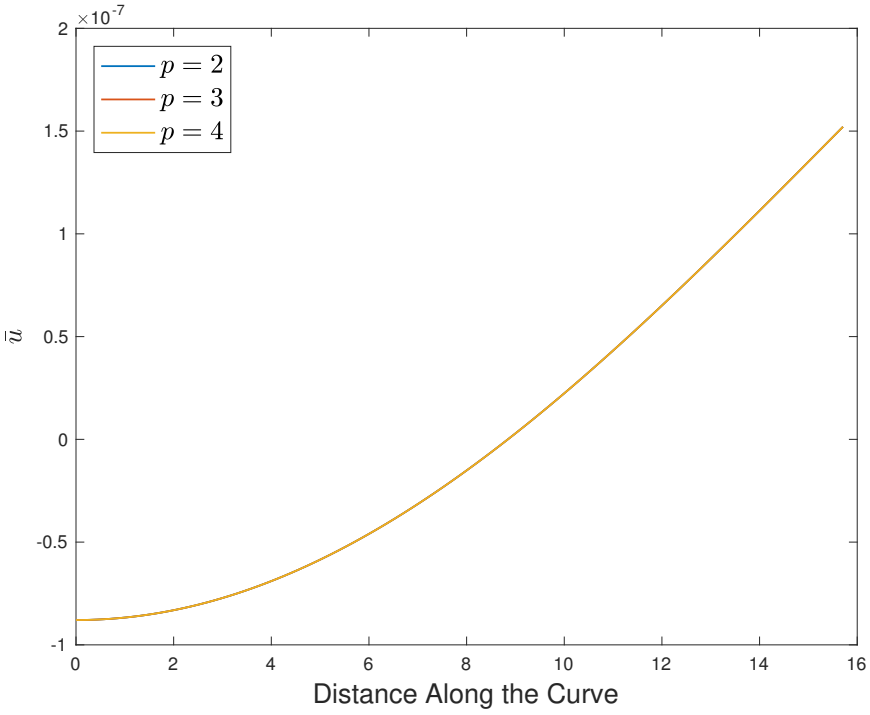

Figure 3.11: The computed TIM MD $\bar{u}$ for shear strain for several degrees and $\frac{R}{t} = 1000$.

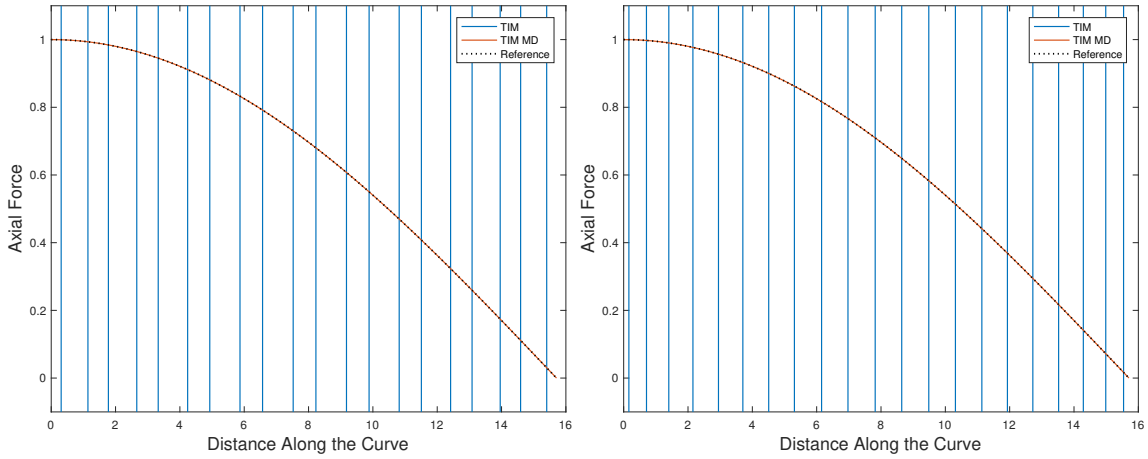

(a) Normalized axial force with $p = 2$ and $\frac{R}{t} = 1000$

(b) Normalized axial force with $p = 3$ and $\frac{R}{t} = 1000$

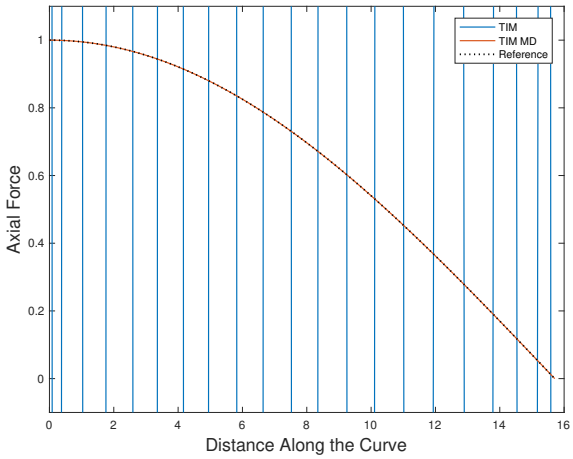

(c) Normalized axial force with $p = 4$ and $\frac{R}{t} = 1000$

Figure 3.12: A comparison of computed axial forces for TIM and TIM MD for different degrees and $\frac{R}{t} = 1000$.

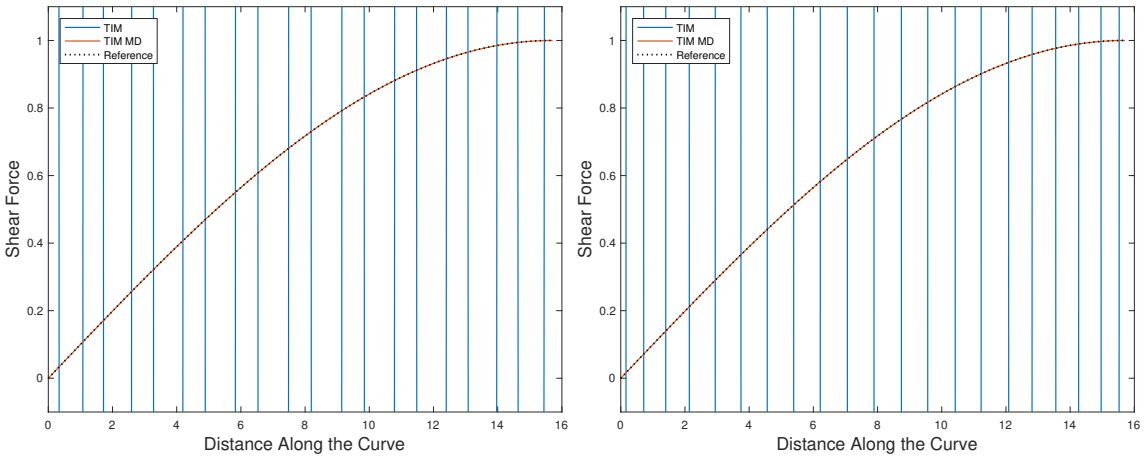

(a) Normalized shear force with $p = 2$ and $\frac{R}{t} = 1000$

(b) Normalized shear force with $p = 3$ and $\frac{R}{t} = 1000$

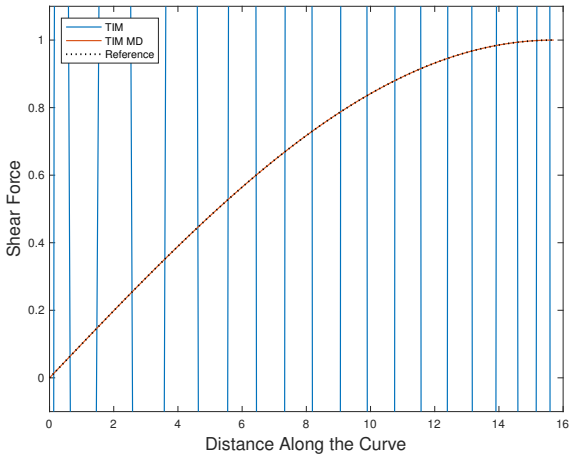

(c) Normalized shear force with $p = 4$ and $\frac{R}{t} = 1000$

Figure 3.13: A comparison of computed shear forces for TIM and TIM MD for different degrees and $\frac{R}{t} = 1000$.

In Figure 3.14, I also look at the number of DOFs needed to achieve the analytic transverse displacement for this last example. Even with the extra fields in the mixed displacement method, the deflection is still calculated with fewer DOFs than the traditional method.

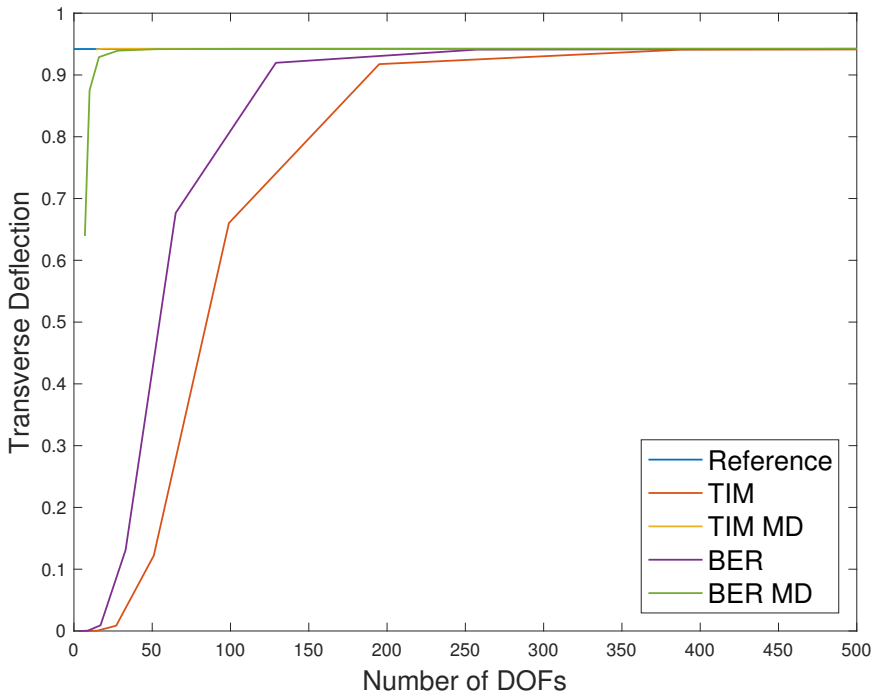

Figure 3.14: The transverse deflection versus the number of DOFs for $p = 2$ and $\frac{R}{t} = 1000$.

CHAPTER 4. CONCLUSION

Blending is capable of eliminating shear locking by taking advantage of the shear locking free behavior of Bernoulli beam over the majority of the beam while still being able to set the rotations by using Timoshenko nodes on the ends of the beam. This was seen in several examples of a straight beam with different boundary conditions. The Hu-Washizu Principle is a more general concept, however. It is able to remove all forms of locking not just shear locking while still being able to provide realistic stresses. This was seen in examples of a curved beam and a straight beam.

The mixed displacement method has not eliminated the need completely for the use of blending. Blending can be used as an optimization method to eliminate DOFs. Eliminating membrane locking in the case of a beam with a curved portion and a straight portion is an example of this. The traditional definition of axial strain over the straight portion can be blended with the modified definition over the curved portion. This would still be locking free, but would not require extra DOFs for the modified strains over the straight portion. Work like this, however, is for the future.

Even though all of the examples presented are for planar beams, the presented methods can be applied to three dimensional beams and shells as well. The planar cases were presented to simplify the exploration of the methods. Blending can be expanded to the general three dimensional theory as the Bernoulli rotation is still written in terms of the derivative of the displacement. The mixed displacement method also can be expanded as one only needs to add a third $\bar{u}$ field to represent the second shear strain.

REFERENCES

[1] Sederberg, T. W., 2014. *Computer Aided Geometric Design*. 1

[2] Borden, M. J., Scott, M. A., Evans, J. A., and Hughes, T. J. R., 2011. "Isogeometric finite element data structures based on bézier extraction of nurbs." *International Journal for Numerical Methods in Engineering,* **87**(1-5), pp. 15–47. 3

[3] Gere, J. M., and Goodno, B. J., 2013. *Mechanics of Materials*. Cengage Learning. 6, 14

[4] Zou, Z., Willoughby, D., Scott, M. A., El-Essawi, M., Baskaran, R., and Alanoly, J., 2017. "A geometrically exact isogeometric blended shell: Formulation, benchmarking, and automotive application." *SAE Int. J. Passeng. Cars - Mech. Syst.,* **10**, 03, pp. 525–533. 8

[5] Oesterle, B., Bieber, S., Ramm, E., and Bishoff, M., 2017. A variational method to avoid locking-independent of the discretization private communication, Apr. 14, 17, 25, 28

[6] Balling, R. J., 2013. *Virtual Work and Flexibility*., Vol. II of *Structural Analysis* BYU Academic Publishing. 15

[7] Belytschko, T., Liu, W. K., Moran, B., and Elkhodary, K. I., 2014. *Nonlinear Finite Elements for Continua and Structures*. Wiley. 17

[8] Hughes, T. J. R., 2000. *The Finite Element Method: Linear Static and Dynamic Finite Element Analysis*. Dover. 38

[9] Bauer, A., Breitenberger, M., Philipp, B., Wüchner, R., and Bletzinger, K.-U., 2016. "Nonlinear isogeometric spatial bernoulli beam." *Computer Methods in Applied Mechanics and Engineering,* **303**, pp. 101–127. 38, 41

APPENDIX A. THREE DIMENSIONAL LINEAR BEAM FORMULATION

The two sources that were heavily consulted in the derivation of this beam theory are [8] and [9].

A.1 A Review of Quaternions

Quaternions can be used as another manner of rotating vectors. They are used as they make it much simpler to reduce equations than rotation matrices. They consist of four numbers, one of which is known as the scalar portion while the other three together are known as the vector portion. I start with some definitions for the general quaternions **a** and **b**, not just rotation quaternions. Remember that $\otimes$ is used to denote the Hamiltonian product instead of the outer product and the functions $V(\mathbf{a})$ and $S(\mathbf{a})$ return the vector portion and the scalar portion of the quaternion **a** respectively. The Hamiltonian product is used to combine quaternions together. There is also the function $Q(\mathbf{v})$ that takes any vector **v** and returns a quaternion whose vector part is the vector **v** and

whose scalar part is zero. The identity quaternion is **e**.

$$V(\mathbf{a}\otimes\mathbf{b}) = V(\mathbf{a})\times V(\mathbf{b}) + S(\mathbf{a})V(\mathbf{b}) + S(\mathbf{b})V(\mathbf{a}) \tag{A.1}$$

$$S(\mathbf{a}\otimes\mathbf{b}) = S(\mathbf{a})S(\mathbf{b}) - V(\mathbf{a})\cdot V(\mathbf{b}) \tag{A.2}$$

$$V(\mathbf{a}\otimes\mathbf{b} - \mathbf{b}\otimes\mathbf{a}) = 2V(\mathbf{a})\times V(\mathbf{b}) \tag{A.3}$$

$$S(\mathbf{a}\otimes\mathbf{b} - \mathbf{b}\otimes\mathbf{a}) = 0 \tag{A.4}$$

$$(\mathbf{a}\otimes\mathbf{b})^{-1} = \mathbf{b}^{-1}\otimes\mathbf{a}^{-1} \tag{A.5}$$

$$\mathbf{e} = \mathbf{a}\otimes\mathbf{a}^{-1} = \mathbf{a}^{-1}\otimes\mathbf{a} \tag{A.6}$$

$$\delta\mathbf{e} = \mathbf{0} = \delta\mathbf{a}\otimes\mathbf{a}^{-1} + \mathbf{a}\otimes\delta\mathbf{a}^{-1} = \delta\mathbf{a}^{-1}\otimes\mathbf{a} + \mathbf{a}^{-1}\otimes\delta\mathbf{a} \tag{A.7}$$

The identities associated with the rotation quaternion **r** and the rotation of the vector $\mathbf{D}_i$ to $\mathbf{d}_i$ can now be presented.

$$\mathbf{d}_i = V(\mathbf{r}\otimes Q(\mathbf{D}_i)\otimes\mathbf{r}^{-1}) \tag{A.8}$$

$$0 = S(\mathbf{r}\otimes Q(\mathbf{D}_i)\otimes\mathbf{r}^{-1}) \tag{A.9}$$

$$V(\mathbf{r}^{-1}) = -V(\mathbf{r}) \tag{A.10}$$

$$S(\mathbf{r}^{-1}) = 0 \tag{A.11}$$

$$1 = S(\mathbf{r})^2 + \|V(\mathbf{r})\|^2 \tag{A.12}$$

$$0 = \delta S(\mathbf{r})S(\mathbf{r}) + \delta V(\mathbf{r})\cdot V(\mathbf{r}) \tag{A.13}$$

$$0 = S(\delta\mathbf{r}\otimes\mathbf{r}^{-1}) \tag{A.14}$$

To finish this review, I now describe what a quaternion means. Another representation of rotations is the rotation vector. I call this vector ω. A quaternion $\mathbf{r}$ in terms of this vector is described in the following.

$$V(\mathbf{r}) = \omega \frac{\sin \frac{\|\omega\|}{2}}{\|\omega\|} \tag{A.15}$$

$$S(\mathbf{r}) = \cos \frac{\|\omega\|}{2} \tag{A.16}$$

A.2 Description of Beam Geometry

The beam is described in terms of the curvilinear coordinate system ξ_i in the following.

$$\tilde{\mathbf{X}}(\xi_1, \xi_2, \xi_3) = \mathbf{X}(\xi_1) + \xi_2 \mathbf{D}_2(\xi_1) + \xi_3 \mathbf{D}_3(\xi_1) \tag{A.17}$$

$$\tilde{\mathbf{x}}(\xi_1, \xi_2, \xi_3) = \mathbf{x}(\xi_1) + \xi_2 \mathbf{d}_2(\xi_1) + \xi_3 \mathbf{d}_3(\xi_1) \tag{A.18}$$

$$\begin{aligned} \tilde{\mathbf{u}}(\xi_1, \xi_2, \xi_3) &= \mathbf{x}(\xi_1, \xi_2, \xi_3) - \mathbf{X}(\xi_1, \xi_2, \xi_3) \\ &= \mathbf{u}(\xi_1) + \xi_2 \Big(\mathbf{d}_2(\xi_1) - \mathbf{D}_2(\xi_1) \Big) + \xi_3 \Big(\mathbf{d}_3(\xi_1) - \mathbf{D}_3(\xi_1) \Big) \\ &= \mathbf{u}(\xi_1) + \xi_2 \Delta \mathbf{d}_2(\xi_1) + \xi_3 \Delta \mathbf{d}_3(\xi_1) \end{aligned} \tag{A.19}$$

A.3 Directors

I now apply the plane sections remain plane assumption. This is done by saying the director $\mathbf{D}_i$ is related to the director $\mathbf{d}_i$ by only a rotation. I also say that $\Delta \mathbf{d}_i$ is just the variation $\delta \mathbf{d}_i$ when $\tilde{\mathbf{u}} = \mathbf{0}$. The rotations are performed with a quaternion $\mathbf{r}$ as it is easier to reduce the resultant

equations.

$$\begin{aligned}\delta\mathbf{d}_i &= \delta V(\mathbf{r}\otimes Q(\mathbf{D}_i)\otimes\mathbf{r}^{-1}) \\ &= V(\delta\mathbf{r}\otimes Q(\mathbf{D}_i)\otimes\mathbf{r}^{-1}+\mathbf{r}\otimes Q(\mathbf{D}_i)\otimes\delta\mathbf{r}^{-1}) \\ &= V(\delta\mathbf{r}\otimes\mathbf{r}^{-1}\otimes\mathbf{r}\otimes Q(\mathbf{D}_i)\otimes\mathbf{r}^{-1}+\mathbf{r}\otimes Q(\mathbf{D}_i)\otimes\mathbf{r}^{-1}\otimes\mathbf{r}\otimes\delta\mathbf{r}^{-1}) \\ &= V((\delta\mathbf{r}\otimes\mathbf{r}^{-1})\otimes Q(\mathbf{d}_i)-Q(\mathbf{d}_i)\otimes(\delta\mathbf{r}\otimes\mathbf{r}^{-1})) \\ &= -\mathbf{d}_i\times V(2\delta\mathbf{r}\otimes\mathbf{r}^{-1})\end{aligned} \tag{A.20}$$

$$\Delta\mathbf{d}_i = -\mathbf{D}_i\times\boldsymbol{\Phi} \tag{A.21}$$

In the above $\boldsymbol{\Phi}$ is defined as $V(2\Delta\mathbf{r}\otimes\mathbf{r}^{-1})$.

A.4 Bernoulli Rotation

This rotation is done by picking a rotation that results in the tangent in the undeformed configuration $\mathbf{T}$ going to the tangent in the deformed configuration $\mathbf{t}$. One option is to rotate about the vector $\mathbf{g}$ that is perpendicular to both tangents through an angle θ [9].

$$\begin{aligned}\mathbf{g} &= \frac{\mathbf{T}\times\mathbf{t}}{\|\mathbf{T}\times\mathbf{t}\|} \\ &= \frac{\mathbf{T}\times\mathbf{t}}{\sin\theta} \\ &= \frac{\mathbf{T}\times\mathbf{t}}{2\sin\frac{\theta}{2}\cos\frac{\theta}{2}}\end{aligned} \tag{A.22}$$

$$\begin{aligned}\cos\frac{\theta}{2} &= \sqrt{\frac{1+\cos\theta}{2}} \\ &= \sqrt{\frac{1+\mathbf{T}\cdot\mathbf{t}}{2}}\end{aligned} \tag{A.23}$$

I also allow the beam to twist about the beam tangent $\mathbf{t}$ through an angle ψ. Combining all of these together, I can say that the final quaternion is the following.

$$V(\mathbf{r}^{BER}) = \sin\frac{\psi}{2}\frac{(\mathbf{T}\times\mathbf{t})\times\mathbf{t}}{\sqrt{2(1+\mathbf{T}\cdot\mathbf{t})}} + \cos\frac{\psi}{2}\frac{\mathbf{T}\times\mathbf{t}}{\sqrt{2(1+\mathbf{T}\cdot\mathbf{t})}} + \sin\frac{\psi}{2}\sqrt{\frac{1+\mathbf{T}\cdot\mathbf{t}}{2}}\mathbf{t} \tag{A.24}$$

$$S(\mathbf{r}^{BER}) = \cos\frac{\psi}{2}\sqrt{\frac{1+\mathbf{T}\cdot\mathbf{t}}{2}} \tag{A.25}$$

Before continuing, I give the definitions of $\mathbf{T}$ and $\mathbf{t}$, as well as the variation of $\mathbf{t}$.

$$\mathbf{T} = \frac{\mathbf{X}_{,1}}{\left\|\mathbf{X}_{,1}\right\|} \tag{A.26}$$

$$\mathbf{t} = \frac{\mathbf{x}_{,1}}{\left\|\mathbf{x}_{,1}\right\|} \tag{A.27}$$

$$\delta\mathbf{t} = \frac{\delta\mathbf{x}_{,1}}{\left\|\mathbf{x}_{,1}\right\|} - \frac{\mathbf{t}(\mathbf{t}\cdot\delta\mathbf{x}_{,1})}{\left\|\mathbf{x}_{,1}\right\|} \tag{A.28}$$

I now take the variation of the quaternion.

$$\begin{aligned}\delta V(\mathbf{r}^{BER}) = {} & \frac{\delta\psi}{2}\cos\frac{\psi}{2}\frac{(\mathbf{T}\times\mathbf{t})\times\mathbf{t}}{\sqrt{2(1+\mathbf{T}\cdot\mathbf{t})}} + \sin\frac{\psi}{2}\delta\frac{(\mathbf{T}\times\mathbf{t})\times\mathbf{t}}{\sqrt{2(1+\mathbf{T}\cdot\mathbf{t})}} \\ & - \frac{\delta\psi}{2}\sin\frac{\psi}{2}\frac{\mathbf{T}\times\mathbf{t}}{\sqrt{2(1+\mathbf{T}\cdot\mathbf{t})}} + \cos\frac{\psi}{2}\frac{\mathbf{T}\times\delta\mathbf{t}}{\sqrt{2(1+\mathbf{T}\cdot\mathbf{t})}} - \cos\frac{\psi}{2}\frac{\mathbf{T}\times\mathbf{t}(\mathbf{T}\cdot\mathbf{t})}{(\sqrt{2(1+\mathbf{T}\cdot\mathbf{t})})^3} \\ & + \frac{\delta\psi}{2}\cos\frac{\psi}{2}\sqrt{\frac{1+\mathbf{T}\cdot\mathbf{t}}{2}}\mathbf{t} + \sin\frac{\psi}{2}\delta\sqrt{\frac{1+\mathbf{T}\cdot\mathbf{t}}{2}}\mathbf{t}\end{aligned} \tag{A.29}$$

$$\delta S(\mathbf{r}^{BER}) = -\frac{\delta\psi}{2}\sin\frac{\psi}{2}\sqrt{\frac{1+\mathbf{T}\cdot\mathbf{t}}{2}} + \cos\frac{\psi}{2}\frac{\mathbf{T}\cdot\delta\mathbf{t}}{2\sqrt{2(1+\mathbf{T}\cdot\mathbf{t})}} \tag{A.30}$$

I can now substitute $\tilde{\mathbf{u}} = \mathbf{0}$ into the above equations.

$$V(\mathbf{r}^{BER}) = \mathbf{0} \tag{A.31}$$

$$S(\mathbf{r}^{BER}) = 1 \tag{A.32}$$

$$\Delta V(\mathbf{r}^{BER}) = \frac{\mathbf{T} \times \Delta \mathbf{t}}{2} + \frac{\Delta \psi}{2}\mathbf{T} \tag{A.33}$$

$$\Delta S(\mathbf{r}^{BER}) = 0 \tag{A.34}$$

I can substitute this into $\mathbf{\Phi}$. I also now recognize that $\Delta \mathbf{x} = \mathbf{u}$ and $\Delta \psi = \psi$ for linear analysis.

$$\mathbf{\Phi}^{BER} = \mathbf{T} \times \frac{\mathbf{u}_{,1}}{\left\|\mathbf{X}_{,1}\right\|} + \psi \mathbf{T} \tag{A.35}$$

A.5 Timoshenko Rotation

This rotation is just a rotation vector $\boldsymbol{\omega}$. In quaternions this is the following.

$$V(\mathbf{r}^{TIM}) = \boldsymbol{\omega} \frac{\sin \frac{\|\boldsymbol{\omega}\|}{2}}{\|\boldsymbol{\omega}\|} \tag{A.36}$$

$$S(\mathbf{r}^{TIM}) = \cos \frac{\|\boldsymbol{\omega}\|}{2} \tag{A.37}$$

Taking the variation of the quaternion, I get the following.

$$\delta V(\mathbf{r}^{TIM}) = \delta \boldsymbol{\omega} \frac{\sin \frac{\|\boldsymbol{\omega}\|}{2}}{\|\boldsymbol{\omega}\|} + \boldsymbol{\omega} \delta \frac{\sin \frac{\|\boldsymbol{\omega}\|}{2}}{\|\boldsymbol{\omega}\|} \tag{A.38}$$

$$\delta S(\mathbf{r}^{TIM}) = \delta \cos \frac{\|\boldsymbol{\omega}\|}{2} \tag{A.39}$$

I now substitute in $\tilde{\mathbf{u}} = \mathbf{0}$. Through the use of Taylor Series Expansions, I can remove $||\omega||$ from the denominator of the above equations as well as reduce them to the following.

$$V(\mathbf{r}^{TIM}) = \mathbf{0} \tag{A.40}$$

$$S(\mathbf{r}^{TIM}) = 1 \tag{A.41}$$

$$\delta V(\mathbf{r}^{TIM}) = \frac{\Delta\omega}{2} \tag{A.42}$$

$$\delta S(\mathbf{r}^{TIM}) = 0 \tag{A.43}$$

I can substitute this into $\mathbf{\Phi}$. I also now recognize that $\Delta\omega = \omega$ for linear analysis.

$$\mathbf{\Phi}^{TIM} = \omega \tag{A.44}$$

A.6 Deformation and Strain

I now substitute this definition for $\Delta\mathbf{d}_i$ back into the definition for the deflection and use that to find the definition for the strain. I use the symmetric gradient definition for strain.

$$\begin{aligned}\tilde{\mathbf{u}} &= \mathbf{u} + \xi_2\Delta\mathbf{d}_2 + \theta\Delta\mathbf{d}_3 \\ &= \mathbf{u} - (\xi_2\mathbf{D}_2 + \xi_3\mathbf{D}_3)\times\mathbf{\Phi}\end{aligned} \tag{A.45}$$

A.6.1 Jacobian

For the strain I need a Jacobian to convert the deflection gradient between the curvilinear coordinates and the rectilinear coordinates. I also rotate the gradient into the local coordinates as

that makes it easier to find the needed Jacobian.

$$\mathbf{Jac}^{-1} = \begin{bmatrix} \mathbf{D}_1^T \\ \mathbf{D}_2^T \\ \mathbf{D}_3^T \end{bmatrix} \begin{bmatrix} \mathbf{X}_{,1} + \xi_2 \mathbf{D}_{2,1} + \xi_3 \mathbf{D}_{3,1} & \mathbf{D}_2 & \mathbf{D}_3 \end{bmatrix} \tag{A.46}$$

$$= \begin{bmatrix} \mathbf{D}_1 \cdot (\mathbf{X}_{,1} + \xi_2 \mathbf{D}_{2,1} + \xi_3 \mathbf{D}_{3,1}) & 0 & 0 \\ \mathbf{D}_2 \cdot (\mathbf{X}_{,1} + \xi_3 \mathbf{D}_{3,1}) & 1 & 0 \\ \mathbf{D}_3 \cdot (\mathbf{X}_{,1} + \xi_2 \mathbf{D}_{2,1}) & 0 & 1 \end{bmatrix}$$

I now invert this matrix using a simple 3x3 inversion rule.

$$Det = \mathbf{D}_1 \cdot (\mathbf{X}_{,1} + \xi_2 \mathbf{D}_{2,1} + \xi_3 \mathbf{D}_{3,1}) \tag{A.47}$$

$$\mathbf{Jac}^{-1} = \begin{bmatrix} \frac{1}{Det} & 0 & 0 \\ \frac{-\mathbf{D}_2 \cdot (\mathbf{X}_{,1} + \xi_3 \mathbf{D}_{3,1})}{Det} & 1 & 0 \\ \frac{-\mathbf{D}_3 \cdot (\mathbf{X}_{,1} + \xi_2 \mathbf{D}_{2,1})}{Det} & 0 & 1 \end{bmatrix} \tag{A.48}$$

A.6.2 Deflection Gradient

I can now find the gradient, remember that the gradient is also being rotated into the local rectilinear coordinate system.

$$\nabla\tilde{\mathbf{u}} = \begin{bmatrix}\mathbf{D}_1^T\\ \mathbf{D}_2^T\\ \mathbf{D}_3^T\end{bmatrix}\left[\mathbf{u}_{,1} - (\xi_2\mathbf{D}_{2,1}+\xi_3\mathbf{D}_{3,1})\times\boldsymbol{\Phi} - (\xi_2\mathbf{D}_2+\xi_3\mathbf{D}_3)\times\boldsymbol{\Phi}_{,1} \quad -\mathbf{D}_2\times\boldsymbol{\Phi} \quad -\mathbf{D}_3\times\boldsymbol{\Phi}\right]\mathbf{Jac} \tag{A.49}$$

$$= \begin{bmatrix} \left(\begin{bmatrix}\mathbf{D}_1^T\\ \mathbf{D}_2^T\\ \mathbf{D}_3^T\end{bmatrix}\mathbf{u}_{,1} + \begin{bmatrix} 0 & \xi_2\mathbf{D}_3\cdot\mathbf{D}_{2,1} & -\xi_3\mathbf{D}_2\cdot\mathbf{D}_{3,1}\\ -\xi_2\mathbf{D}_3\cdot\mathbf{D}_{2,1} & 0 & \mathbf{D}_1\cdot(\xi_2\mathbf{D}_{2,1}+\xi_3\mathbf{D}_{3,1})\\ \xi_3\mathbf{D}_2\cdot\mathbf{D}_{3,1} & -\mathbf{D}_1\cdot(\xi_2\mathbf{D}_{2,1}+\xi_3\mathbf{D}_{3,1}) & 0\end{bmatrix}\begin{bmatrix}\mathbf{D}_1^T\\ \mathbf{D}_2^T\\ \mathbf{D}_3^T\end{bmatrix}\boldsymbol{\Phi} + \begin{bmatrix} 0 & \xi_3 & -\xi_2\\ -\xi_3 & 0 & 0\\ \xi_2 & 0 & 0\end{bmatrix}\begin{bmatrix}\mathbf{D}_1^T\\ \mathbf{D}_2^T\\ \mathbf{D}_3^T\end{bmatrix}\boldsymbol{\Phi}_{,1}\right)^T \\ \left(\begin{bmatrix} 0 & 0 & -1\\ 0 & 0 & 0\\ 1 & 0 & 0\end{bmatrix}\begin{bmatrix}\mathbf{D}_1^T\\ \mathbf{D}_2^T\\ \mathbf{D}_3^T\end{bmatrix}\boldsymbol{\Phi}\right)^T \\ \left(\begin{bmatrix} 0 & 1 & 0\\ -1 & 0 & 0\\ 0 & 0 & 0\end{bmatrix}\begin{bmatrix}\mathbf{D}_1^T\\ \mathbf{D}_2^T\\ \mathbf{D}_3^T\end{bmatrix}\boldsymbol{\Phi}\right)^T \end{bmatrix}$$

$$* \begin{bmatrix} \frac{1}{Det} & 0 & 0\\ \frac{-\mathbf{D}_2\cdot(\mathbf{X}_{,1}+\xi_3\mathbf{D}_{3,1})}{Det} & 1 & 0\\ \frac{-\mathbf{D}_3\cdot(\mathbf{X}_{,1}+\xi_2\mathbf{D}_{2,1})}{Det} & 0 & 1\end{bmatrix}$$

$$= \begin{bmatrix} \frac{1}{Det}\left(D\mathbf{u}_{,1} + \begin{bmatrix} 0 & -\mathbf{D}_3\cdot\mathbf{X}_{,1} & \mathbf{D}_2\cdot\mathbf{X}_{,1}\\ \mathbf{D}_3\cdot\mathbf{X}_{,1} & 0 & Det-\mathbf{D}_1\cdot\mathbf{X}_{,1}\\ -\mathbf{D}_2\cdot\mathbf{X}_{,1} & -Det+\mathbf{D}_1\cdot\mathbf{X}_{,1} & 0\end{bmatrix}\begin{bmatrix}\mathbf{D}_1^T\\ \mathbf{D}_2^T\\ \mathbf{D}_3^T\end{bmatrix}\boldsymbol{\Phi} + \begin{bmatrix} 0 & \xi_3 & -\xi_2\\ -\xi_3 & 0 & 0\\ \xi_2 & 0 & 0\end{bmatrix}\begin{bmatrix}\mathbf{D}_1^T\\ \mathbf{D}_2^T\\ \mathbf{D}_3^T\end{bmatrix}\boldsymbol{\Phi}_{,1}\right)^T \\ \left(\begin{bmatrix} 0 & 0 & -1\\ 0 & 0 & 0\\ 1 & 0 & 0\end{bmatrix}\begin{bmatrix}\mathbf{D}_1^T\\ \mathbf{D}_2^T\\ \mathbf{D}_3^T\end{bmatrix}\boldsymbol{\Phi}\right)^T \\ \left(\begin{bmatrix} 0 & 1 & 0\\ -1 & 0 & 0\\ 0 & 0 & 0\end{bmatrix}\begin{bmatrix}\mathbf{D}_1^T\\ \mathbf{D}_2^T\\ \mathbf{D}_3^T\end{bmatrix}\boldsymbol{\Phi}\right)^T \end{bmatrix}$$

A.6.3 Strain

The definition of strain is as follows.

$$\boldsymbol{\epsilon} = \frac{1}{2}(\nabla\tilde{\mathbf{u}} + \nabla\tilde{\mathbf{u}}^T) \tag{A.50}$$

Using this definition it can be seen that the components of the strain are equal to the following.

$$\epsilon_{22} = \epsilon_{33} = \epsilon_{23} = 0 \tag{A.51}$$

$$\begin{bmatrix} \epsilon_{11} \\ 2\epsilon_{12} \\ 2\epsilon_{13} \end{bmatrix} = \frac{1}{Det} \begin{bmatrix} 1 & 0 & 0 & 0 & \xi_3 & -\xi_2 \\ 0 & 1 & 0 & -\xi_3 & 0 & 0 \\ 0 & 0 & 1 & \xi_2 & 0 & 0 \end{bmatrix} \begin{bmatrix} \mathbf{D}_1 \cdot (\mathbf{u}_{,1} + \mathbf{X}_{,1} \times \mathbf{\Phi}) \\ \mathbf{D}_2 \cdot (\mathbf{u}_{,1} + \mathbf{X}_{,1} \times \mathbf{\Phi}) \\ \mathbf{D}_3 \cdot (\mathbf{u}_{,1} + \mathbf{X}_{,1} \times \mathbf{\Phi}) \\ \mathbf{D}_1 \cdot \mathbf{\Phi}_{,1} \\ \mathbf{D}_2 \cdot \mathbf{\Phi}_{,1} \\ \mathbf{D}_3 \cdot \mathbf{\Phi}_{,1} \end{bmatrix} \tag{A.52}$$

A.7 Resultant Based Beam

I am now ready to convert this into a resultant based beam. **D** is the matrix of material moduli. This matrix has already been modified to comply with the plane stress assumption, however, I will not go into the details of this. The beam strains $\boldsymbol{\varepsilon}$ are defined as follows

$$\boldsymbol{\varepsilon} = \begin{bmatrix} \mathbf{D}_1 \cdot (\mathbf{u}_{,1} + \mathbf{X}_{,1} \times \mathbf{\Phi}) \\ \mathbf{D}_2 \cdot (\mathbf{u}_{,1} + \mathbf{X}_{,1} \times \mathbf{\Phi}) \\ \mathbf{D}_3 \cdot (\mathbf{u}_{,1} + \mathbf{X}_{,1} \times \mathbf{\Phi}) \\ \mathbf{D}_1 \cdot \mathbf{\Phi}_{,1} \\ \mathbf{D}_2 \cdot \mathbf{\Phi}_{,1} \\ \mathbf{D}_3 \cdot \mathbf{\Phi}_{,1} \end{bmatrix} \tag{A.53}$$

and the beam stiffness parameters **C** are defined as follows

$$\mathbf{C} = \int_A \frac{1}{Det} \begin{bmatrix} 1 & 0 & 0 & 0 & \xi_3 & -\xi_2 \\ 0 & 1 & 0 & -\xi_3 & 0 & 0 \\ 0 & 0 & 1 & \xi_2 & 0 & 0 \end{bmatrix}^T \mathbf{D} \begin{bmatrix} 1 & 0 & 0 & 0 & \xi_3 & -\xi_2 \\ 0 & 1 & 0 & -\xi_3 & 0 & 0 \\ 0 & 0 & 1 & \xi_2 & 0 & 0 \end{bmatrix} dA \tag{A.54}$$

From here I can say that the beam resultant stresses $\boldsymbol{\sigma}$ are

$$\boldsymbol{\sigma} = \mathbf{C}\boldsymbol{\varepsilon} \tag{A.55}$$

A.8 Reducing to a Planar Beam

A planar beam is very special in that its geometry and deflection are only in a plane. I assume that that plane is the plane perpendicular to the Z-axis and that the Z-axis corresponds with $\mathbf{D}_3$. All rotations and moments must also be about the Z-axis while all displacements and forces must be in the plane. I also assume that the curve $\mathbf{X}$ passes through the centroid and is orthogonal to the cross section. I also assume that $\mathbf{D}_2$ and $\mathbf{D}_3$ are aligned with the principal axes. The last modification is that the derivatives are converted to be with respect to s instead of the parameter ξ_1. All of this results in the following vector of strains

$$\boldsymbol{\varepsilon} = \begin{bmatrix} \varepsilon \\ \gamma \\ \kappa \end{bmatrix} = \begin{bmatrix} \mathbf{D}_1 \cdot \mathbf{u}_{,1} \\ \mathbf{D}_2 \cdot \mathbf{u}_{,1} - \phi \\ \phi_{,s} \end{bmatrix} \tag{A.56}$$

$$\mathbf{C} = \begin{bmatrix} EA & 0 & 0 \\ 0 & GA & 0 \\ 0 & 0 & EI \end{bmatrix} \tag{A.57}$$

These are now in the form that was seen throughout the rest of the thesis.